RISK ASSESSMENT OF SARS-COV-2 DUE TO RESPIRATORY DROPLET TRANSMISSION INSIDE AN ELEVATOR UNDER VARIOUS CLIMATIC CONDITIONS AND VENTILATION SCENARIOS

THESIS SUBMITTED IN PARTIAL FULFILMENTS OF THE REQUIREMENT FOR THE DEGREE OF MASTER OF ENGINEERING IN MECHANICAL ENGINEERING UNDER FACULTY OF ENGINEERING AND TECHNOLOGY

Submitted by

ANISH PAL

Class Roll Number: 002011202004
Registration No.: 131748 of 2015-16
Exam Roll No.: M4MEC22004
Academic Session: 2020-2022

Under the guidance of
Prof. Sourav Sarkar
&
Prof. Achintya Mukhopadhyay
Department of Mechanical Engineering
Jadavpur University

DECLARATION OF ORIGINALITY AND COMPLIANCE OF ACADEMIC ETHICS

I hereby declare that the thesis entitled "**RISK ASSESSMENT OF SARS-COV-2 DUE TO RESPIRATORY DROPLET TRANSMISSION INSIDE AN ELEVATOR UNDER VARIOUS CLIMATIC CONDITIONS AND VENTILATION SCENARIOS**" contains literature survey and original research work by the undersigned candidate, as a part of his *MASTER OF ENGINEERING IN MECHANICAL ENGINEERING under the DEPARTMENT OF MECHANICAL ENGINNERING*, studies during academic session 2020-2022.

All information in this document have been obtained and presented in accordance with the academic rules and ethical conduct.

I also declare that, as required by these rules of conduct, I have fully cited and referenced all the material and results that are not original to this work.

Name: **ANISH PAL**

Class Roll Number: **002011202004**

University Registration No: **131748 of 2015-16**

Examination Roll No: **M4MEC22004**

Date:

Signature:

FACULTY OF ENGINEERING & TECHNOLOGY

DEPARTMENT OF MECHANICAL ENGINEERING

JADAVPUR UNIVERSITY

KOLKATA-700032

CERTIFICATE OF RECOMMENDATION

This is to certify that the thesis entitled "**RISK ASSESSMENT OF SARS-COV-2 DUE TO RESPIRATORY DROPLET TRANSMISSION INSIDE AN ELEVATOR UNDER VARIOUS CLIMATIC CONDITIONS AND VENTILATION SCENARIOS**" is a bonafide work carried out by ANISH PAL under our supervision and guidance in partial fulfilment of the requirements for awarding the degree of Master of Engineering in Mechanical Engineering under Department of Mechanical Engineering, Jadavpur University during the academic session, 2020-2022.

THESIS SUPERVISOR
Prof. Sourav Sarkar
Assistant Professor
Department of Mechanical Engineering
Jadavpur University, Kolkata

THESIS SUPERVISOR
Prof. Achintya Mukhopadhyay
Professor
Department of Mechanical Engineering
Jadavpur University, Kolkata

Prof. Chandan Mazumdar
Dean
Faculty Council of Engineering and Technology
Jadavpur University, Kolkata

Prof. Amit Karmakar
Head of Department
Department of Mechanical Engineering
Jadavpur University, Kolkata

FACULTY OF ENGINEERING & TECHNOLOGY

DEPARTMENT OF MECHANICAL ENGINEERING

JADAVPUR UNIVERSITY

KOLKATA-700032

CERTIFICATE OF APPROVAL

The foregoing thesis, entitled "**RISK ASSESSMENT OF SARS-COV-2 DUE TO RESPIRATORY DROPLET TRANSMISSION INSIDE AN ELEVATOR UNDER VARIOUS CLIMATIC CONDITIONS AND VENTILATION SCENARIOS**" is hereby approved as a creditable study in the area of Mechanical Engineering carried out and presented by ANISH PAL in a satisfactory manner to warrant its acceptance as a prerequisite to the degree for which it has been submitted. It is notified to be understood that by this approval, the undersigned do not necessarily endorse or approve any statement made, opinion expressed and conclusion drawn therein but approve the thesis only for the purpose for which it has been submitted

Committee of final evaluation of thesis:

Signature of Examiners

ACKNOWLEDGEMENT

I would like to record here my gratitude to all who supported me and gave constructive suggestions during the completion of this work.

Separately, I express my deepest gratitude to **Prof. Sourav Sarkar Sir**, Assistant Professor, Department of Mechanical Engineering and co-supervisor **Prof. Achintya Mukhopadhyay Sir**, Professor, Department of Mechanical Engineering, for their invaluable guidance. The regular discussions and idea-sharing with my thesis supervisors really helped me to improve my knowledge day by day my research related problems. At the beginning of this work, they gave me the valuable instruction that properly guided me in right path to accomplish this paper. It was really a pleasure work under their supervision.

I sincerely believe that I was fortunate enough to have come across **Prof. Sourav Sarkar Sir**, who can inspire someone to work wonders. It would really have been not possible for me to complete this thesis without his assistance, proper guidance and motivation. He always helped me during the critical phase of this thesis and was always available for me for any query, whether it's a telephonic or a face to face discussion. Above all he enhanced my confidence and guided me throughout my work.

I would also like to sincerely thank, **Mr. Riddhideep Biswas**, UG-IV, Department of Mechanical Engineering for helping me to carry out this research work.

I would like to thank **Prof. Aranyak Chakravarty Sir**, Assistant Professor, School of Nuclear Studies and Application, for his valuable time and sharing very important insights related to my research work.

I would also like to express my gratitude to the **High Performance Computing Cluster at Jadavpur University's Technological Bhavan** for helping me to complete the simulations in a timely manner.

I am highly indebted to all my professors, their guidance and supervision as well as for providing necessary information regarding thesis and also for their support in completing my master's thesis.

I would like to express my gratitude towards my parents for their kind cooperation and encouragement which helped me in the completion of my master's thesis.

Finally, my thanks and appreciations also go to my dear friends in developing my master's project and people who have willingly helped me out with their abilities.

ANISH PAL

M.E ("Mechanical Engineering")

2nd Year, Final Semester

Department of Mechanical Engineering

Jadavpur University, Kolkata

Publication Details:

1. R.Biswas, A.Pal , R.Pal, S. Sarkar, A.Mukhopadhyay, Risk assessment of COVID infection by respiratory droplets from cough for various ventilation scenarios inside an elevator: An OpenFOAM-based computational fluid dynamics analysis, Physics of Fluids, 34(2022).
2. A.Pal , R.Biswas, S. Sarkar, A.Mukhopadhyay A comprehensive analysis of the effect of ventilation and climatic conditions on covid-19 transmission through respiratory droplet transport via both airborne and fomite mode inside an elevator, (under-review- Physics of Fluids)(https://arxiv.org/abs/2205.11281).

TABLE OF CONTENTS

NOMENCLATURE	
C_p	Specific heat capacity of Eulerian phase (air) ($Jkg^{-1}K^{-1}$)
$C_{p,d}$	Specific heat capacity of droplet ($Jkg^{-1}K^{-1}$)
C_d	Coefficient of drag
d_d	Diameter of droplet (m)
D_{eff}	Effective diffusivity (m^2s^{-1})
D_{mol}	Molecular diffusivity in air (m^2s^{-1})
F_{lift}	Lift force on droplets(N)
f_v	Mass fraction of water vapour in Eulerian phase
H	Enthalpy (Jkg^{-1})
h	Convective heat transfer coefficient ($Wm^{-2}K^{-1}$)
h_{fg}	Latent heat of vaporisation of droplet (Jkg^{-1})
k	Turbulent kinetic energy (Jkg^{-1})
k_{mt}	Mass transfer coefficient for droplet (ms^{-1})
m_d	Mass of droplet (kg)
p	Static pressure of Eulerian phase (Nm^{-2})
P	Turbulent kinetic energy production ($Nm^{-2}s^{-1}$)
RH	Relative humidity (percentage)
T	Temperature (K)
T_d	Temperature of droplet (K)
$\vec{u}$	Velocity of the Eulerian phase (ms^{-1})
$\overrightarrow{u_d}$	Velocity of droplet (ms^{-1})
ρ	Density of Eulerian phase (kgm^{-3})
Y_d^s	Mass fraction of non-volatile component of droplet
Y_d^l	Mass fraction of volatile component of droplet
ρ_d	Density of droplet (kgm^{-3})
m_d^0	Initial mass of droplet (kg)
$C_{p,s}$	Specific heat capacity of non-volatile component of droplet ($Jkg^{-1}K^{-1}$)

$C_{p,l}$	Specific heat capacity of volatile component of droplet ($Jkg^{-1}K^{-1}$)
t	Time (s)
μ	Dynamic viscosity of Eulerian phase ($kgm^{-1}s^{-1}$)
μ_t	Turbulent viscosity of Eulerian phase ($kgm^{-1}s^{-1}$)
Y_0^S	Initial mass fraction of non-volatile component of droplet
m_{wl}	Molecular wt. of volatile component in droplet(kg)
Sh	Sherwood number
Nu	Nusselt number

List of Figures

List of Tables

ABSTRACT

Respiratory droplets that carry the disease-causing virus and are exhaled when speaking, coughing, or sneezing are one of the major causes of the worldwide Covid-19 epidemic. The risks of disease transmission due to these droplets are significantly high in confined public spaces like elevators. A numerical analysis using OpenFOAM has been performed in this work to investigate the droplet dispersion routes in an enclosed environment resembling an elevator. The effect of three ventilation scenarios on droplet dispersal, namely the quiescent, Exhaust Fan and the fan-driven ventilation, both subjected to various climatic conditions (of temperature and humidity) ranging from cold-humid (15°C, 70% relative humidity) to hot-dry (30°C, 30% relative humidity and 30°C, 50% relative humidity) and hot-humid (30°C, 70% relative humidity) have been studied. A risk factor derived from a dose response model based on the time-averaged pathogen quantity present in a typical breathing box around the passenger's mouth is used to quantify the risk of infection through airborne mode. It is found that the hot, dry quiescent scenario poses the greatest threat of infection (spatio-averaged risk factor 42% over the exposure time of elevator travel time), whereas the cold humid condition poses the least risk of infection (spatio-averaged risk factor 30%). The exhaust fan is the ventilation scenario is the best one since it helps the droplets to escape out of the domain very quickly and thus reduces infection risk significantly. The proper Fan speed is determined for the epidemiologically safe operation of the elevator. The implementation of Fan ventilation at low RPM increases the risk as compared to a quiescent scenario, however with the increase in speed the risk decreases significantly. The Fan ventilation scenario with 1100 RPM (having a spatio-averaged risk factor of 10%) decreases the risk of infection by 67% in a hot, dry climatic condition as compared to a quiescent scenario. However, there is no significant reduction in risk beyond a certain Fan speed,1100 RPM. This Fan ventilation scenario (1100 RPM) is seen to sustain similar low risk irrespective of climatic variations. The humidity is discerned to emerge as 10 times more important factor in deciding the risk as compared to temperature. Besides the airborne-mode of infection, the fomite mode of infection (infection through touch) has also been investigated for both the ventilation scenarios. Apposite

curative strategies to evade both forms of risk are formulated for both the ventilation scenarios. A minimum period of 2.5 seconds is determined, after which the elevator can be safely used after a COVID infected person has contaminated it.

Chapter 1

INTRODUCTION

The ongoing pandemic of Covid-19 has caused an immense loss of lives as well as shattered the global economy, the entire world still suffering from its excruciating shackles. Figure 1(a)-(b) the confirmed covid-19 cases in various countries across the world as well as their corresponding fatality rates as of June, 2022[1].

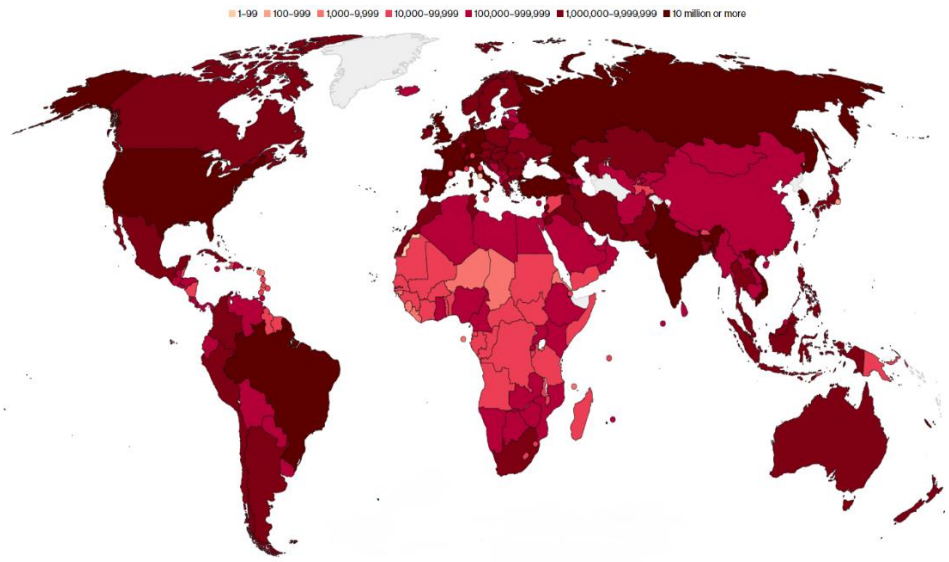

(a)

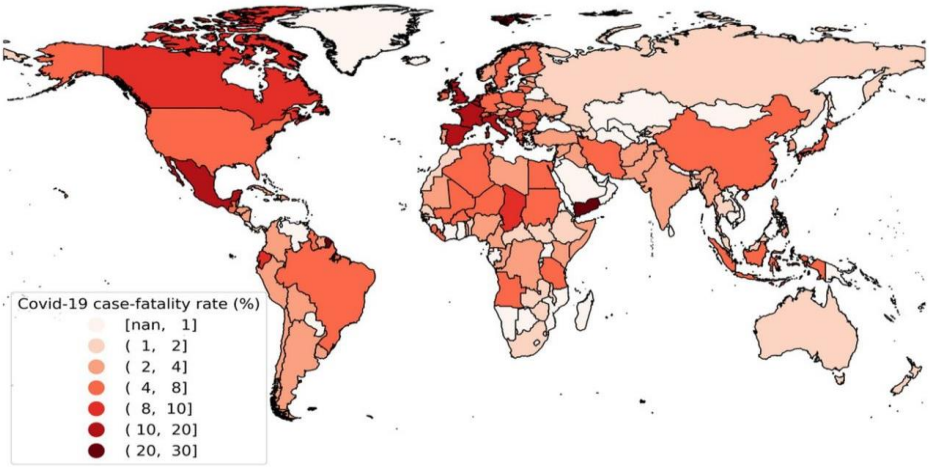

(b)

Figure 1(a)-(b): Contour map showing covid-19 cases and fatality rate over the world (June 2022) [1].

As of June, 2022 approximately 534 million covid cases has been reported and 6 million deaths has occurred due to the pandemic. But, besides causing the immense human loss to the world it also has jolted the world economy. Figure 2 paints the grim picture of the world economy since the pandemic hit the world[2].

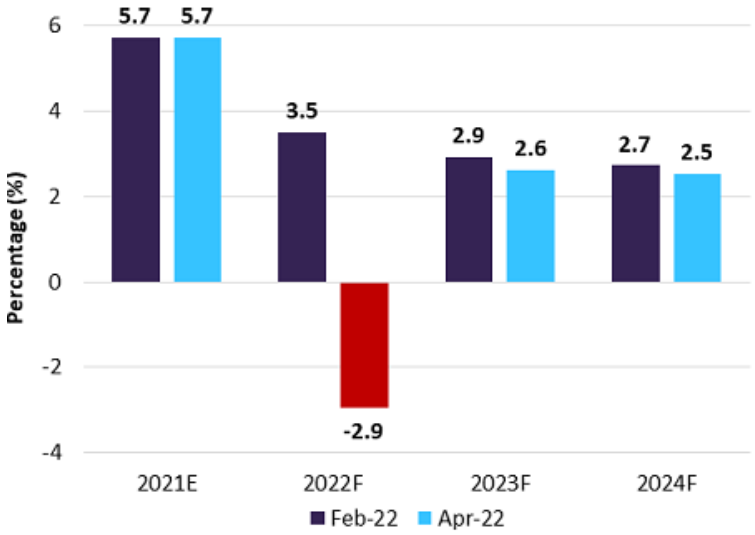

Figure 2: Impact of Covid-19 on global GDP growth[2]

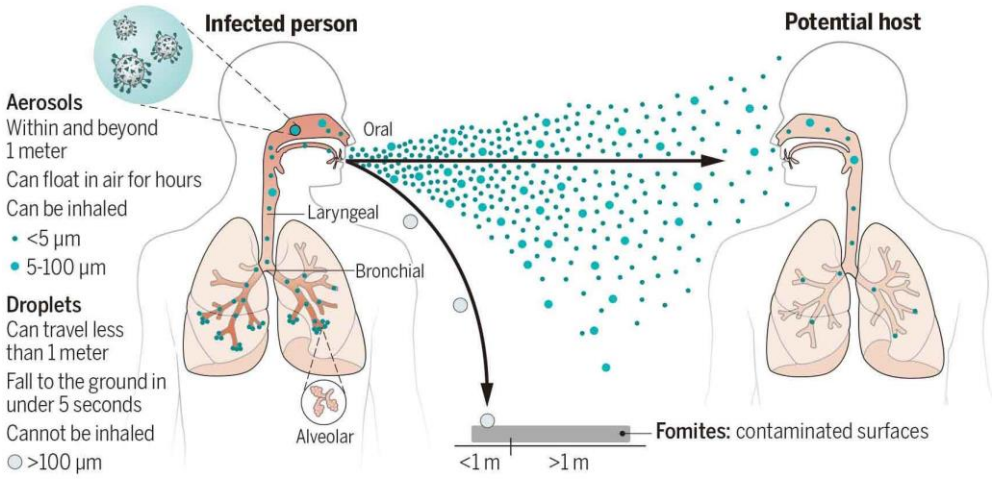

Figure 3: Illustration showing both airborne and fomite mode of Covid transmission[3].

The transmission of Sars-Cov-2 through respiratory droplets has played a major role for this transgression [4,5]. Droplets are ejected during various respiratory activities like breathing, coughing, speaking and singing, dispersal of which causes disease transmission. Figure 3 provides an illustration how covid-19 spreads through both airborne and fomite mode via respiratory droplets[3]. Droplets are generated from both the lower part (bronchial and alveolar) and upper part (Extrathoracic) of the as has been depicted in Fig. 3. The droplets that linger in the domain form the pathway for airborne transmission and those settle down on surface provide a pathway of fomite mode of infection transmission (infection by touch). A number of volatile and non-volatile components dissolved in water constitute a spherical respiratory droplet[6]. Understanding the droplet dispersal is important for developing apposite evasive strategies that ensures minimum infection risk. Dissemination of droplets depends on a number of factors involving prevailing air flow in the domain where the droplets are being injected, the climatic ambience, the droplet size and the thermophysical properties of the droplets[7]. A deeper look into the mechanisms of droplet dispersion divulges droplet dispersal is nothing but transport of one fluid within another fluid medium which turns out to be an age old area of study in the domain of thermos-fluid sciences [7]. Herein, lies the role of a mechanical engineer in contributing towards the world's fight against the pandemic in prescribing solutions based on the understanding of fluid mechanics and heat transfer that mitigates disease transmission.

1.1. Motivation

The understanding that droplet dissemination is at its core a multiphase flow opens up multitudinous approaches to analyse the issue. Several well established numerical frameworks exist that provide a detailed analysis pertaining to multiphase flow[8,9]. In this particular aspect implementing a eulerian-lagrangian framework to model the dynamics and the thermodynamical aspects of a discrete number of particles in another fluid domain suffices the investigation of respiratory-droplet dynamics[10]. The climatic ambiences and ventilation conditions greatly impact the droplet dynamics and the associated heat-transfer. The climatic ambiences mainly impact the droplet heat-transfer which finally control the droplet size which

greatly impacts the droplet trajectory. Furthermore, the existing ventilation conditions control the airflow which ultimately controls the droplet dynamics in the domain. The results of such investigates will contribute towards the worlds fight to minimize both humanitarian and economic losses associated with the pandemic by providing apposite strategies. These outcomes associated with these investigations necessitates this study.

1.2. Overview

- **Respiratory Droplets**

Various respiratory activities like speaking, coughing, sneezing, singing and breathing generate respiratory droplets[11,12]. Depending upon the respiratory activities droplet sizes vary considerably[13]. Droplet sizes vary from the sub-micron range to a few-hundred microns[13]. The size of ejected droplets greatly influence the droplet trajectories which ultimately controls the risk transmission. The droplets with larger masses descend quickly whereas the smaller droplet remain suspended in domain for extended period posing a significant risk[14]. Also, it must be noted that droplets settling on surface pose a fomite infection pathway. The pathogen concentration in the respiratory fluids vary with the region from which the respiratory droplets are generated[15,16]. The pathogen concentration besides the quantity of droplets inhaled plays a major role in the infection probability of a susceptible person. Hence the risk formulations would vary with various respiratory activities since not only the droplet dynamics varies but also the pathogen concentration.

The risk formulation requires tracking of each individual respiratory droplet ejected into them. Thus this requires treating each individual droplet as a separate entity and analysis both its trajectory and heat-transfer characteristics since both aspects controls whether the droplets would settle down or continue to linger in the domain. A Eulerian-Lagrangian solver that takes into account each respiratory droplet as a separate entity suits the requirement. The Eulerian-Langrangian solver solves the droplets in lagrangian phase as discrete particles solving their trajectories and associated heat-transfer. The fluid medium which nests these droplets is solved in the eulerian phase.

- **Eulerian-Lagrangian Solver (OpenFoam)**

1. Eulerian Phase

The Eulerian part of the solver describes the nonreacting chemical and thermodynamic equilibrium flow of the gas mixture through the continuity, momentum and energy equations. Individual transport of the mixture components is accounted through the motion of mixture with the mass-averaged velocity and relative movement of components through the diffusion mechanism. The influence of the dispersed phase on the continuous phase is accounted via source terms in the balance equations of mass, energy, and momentum.

2. Lagrangian Phase

The model of the liquid-droplet system is based on the OpenFOAM[9] cloud model formulated using the Lagrangian approach. Within this model, a system of liquid droplets is represented as a cloud of so-called parcels or bundles of droplets with similar mass. Such representation allows us to save computational resources for real applications in which the resolution of each droplet is not feasible (the total number of particles is larger than 10^7)[17]. Each parcel is characterized by the geometric centre of masses x_p of spherical particles with diameter D_p, density ρ_p, mass $m_p = \frac{1}{6}\rho_p \pi D_p^3$, temperature T_p, and velocity Up. The evolution of each particle is governed by kinematic Equation, momentum-balance Equation, mass-balance Equation, and energy-balance Equation. The momentum, mass-balance and energy equation is solved for every parcel. The temperature, mass-fraction of the droplet components, the co-ordinates and velocity of each parcel is individually solved. During the motion, particles interact with the gas flow and exchange mass, momentum, and energy via processes of viscous drag, heating, and evaporation. The energy and mass between the phases is estimated using semiempirical closure relations.

Researchers have investigated the dispersion of droplets in both outdoor and indoor settings and tried to discern the implications of various factors on droplet dissemination.

1.3. Literature data on droplet dispersion in Outdoor Setting

If a person is present in an open area like a school ground or market place, the risk of the disease transmission depends on wind velocity due to the available space between two persons. Feng et al. carried out a numerical study to investigate the effects of wind and relative humidity on the transportation of respiratory droplets in an outdoor environment for different wind velocity ranges from 0-16 km/h[18]. They have found that the droplet cloud can travel up to 8 m in the presence of wind. Li et al. performed numerical study on dispersion of cough droplets with non-volatile components in a tropical outdoor environment and the dispersion was influenced by the relative humidity and wind speed[19]. Yang et al. studied the effect of window velocity on body thermal plume, and eventually the droplet dispersion. They further investigated the effect of window velocity and relative humidity on social distancing that need to be maintained for ensuring minimum infection risk. They concluded that not only proper social distancing is necessary but also proper angle with the wind velocity is important[20]. Maggiore et al. numerically investigated the droplet generated from breathing and light cough and its dispersal in an outdoor environment. They investigated their evaporation characteristics and droplet dynamics for various pressure, relative humidity (R.H.), temperature and tried to determine proper social distances that needs to be maintained[21]. Aydin et al. determined the maximum distance a single virus can travel under various combinations of droplet size, wind speed and falling time. They concluded that both droplet size and wind speed have a significant impact on the droplet travel. Furthermore, they carried out the investigation at various instants of a day (mid-day, mid-night) and obtained different results based on the instance the investigation was being carried out[22]. Li et al. implemented a Eulerian-Lagrangian framework to study the impact of coughing intensity and wind velocity on the dispersion of droplet velocity. They concluded that in the event of strong coughing also the droplets do not disperse far in an ambient air with no wind however the spread increased significantly in the presence of a wind. Furthermore, it was discovered the direction of wind velocity has a significant impact as well[23]. Hetherington et al. conducted an exposure risk analysis of COVID-19 for a ride-sharing motorbike taxi, and determined that based on the

bike speed and droplet size the infection risk varies and concluded that shield provides sufficient protection and mitigates the risk[24]. Dbouk et al. reported that the pollens can capture the coronavirus and transmit to long distances thus ultimately increasing the risk of infection. Furthermore, in the presence of a prevailing wind the pollen can travel large distances thus requiring revising the social distance rule in the month of spring when pollination takes place[25].

In an open space, it has been observed from the above literatures that the wind speed, the relative humidity, coughing intensity, wind direction, temperature and droplet size affect the droplet size affect the droplet dispersion. However, through appropriate social distancing the infection risk can maintained at a minimal level. On the other hand, the situation becomes alarming in an indoor scenario where maintaining proper social distancing is not possible and droplets remain suspended in the domain for considerable periods. Furthermore, many a times an indoor setting has poor ventilation which further compounds the issue as the virus cannot escape the domain. Hence investigation of droplet transmission in an indoor setting is very important as droplet dispersal in an enclosed domain poses a very high risk.

1.4. Literature data on droplet dispersion in indoor Setting

Several investigations on droplet or aerosol dispersion in confined settings, such as classrooms[26–29], airline cabins[30], restaurants[31], buses[32–35], clinics[36,37], car cabin[38] and courtroom[39] have recently been conducted. Cammarata et al. studied dynamic evaluation of the risk of viral infection in air[40]. Venkatram et al. used eddy diffusivity to model turbulent aerosol movement inside rooms[41]. Dbouk et al. demonstrated how changes in ventilation settings in enclosed places might affect airborne viral transmission[10]. Sen examined the transmitting of cough droplets in an enclosed domain such as a lift, taking into account a number of variables such as ventilation settings, the individual count within the elevator, the discharge direction, humidity level, and temperature[7]. Drivas et al. developed an analytical model that helps in assessing the human health risk from short-term indoor contaminants[42]. Xie et al. determined how far droplets can traverse in indoor environments[43]. Miller et al. investigated the superspreading event of

Skagit Valley Chorale[44]. Ai et al. examined the spread of expiratory droplet nuclei in an indoor environment[45]. Pal et al. studied the effect of climatic conditions on the dispersion of droplets in an indoor ambiance[14]. The droplet trajectories are determined for different ambient temperatures and relative humilities. Cheng et al. examined the paths of big respiratory droplets in different relative humidity in indoor environments[46]. The viral load dependency of the residence periods of virus-laden droplets from COVID-19-infected patients in indoor settings was studied by Srinivasan et al.[47].

Table 1, below summarizes the above-discussed works in indoor-settings, outdoor-settings as well as the studies that implemented wells-riley and dose response model for risk quantification.

Table 1: Summary of Literature data

SR No.	Authors	Analysis
Outdoor Settings		
1	Feng et al. [18].	Droplet transport for wind velocity range, 0-16 km/h.
2	Li et al. [19].	Dispersal of cough droplets in various R.H. and wind velocity.
3	Yang et al. [20].	Wind velocity, Social Distance, Wind direction, R.H. effect on wind velocity.
4	Maggiore et al.[21].	Evaporation Characteristics and droplet dynamics for various pressure, temperature, and R.H.
5	Aydin et al. [22].	Maximum distance a single virus can travel under various combinations of droplet size, wind speed and falling time.
6	Li et al. [23].	Impact of coughing intensity and wind direction on droplet dispersal.
7	Hetherington et al. [24].	Risk analysis of a motorbike taxi for various bike speeds.
8	Dbouk et al. [25].	Dispersal of droplets through pollens.

Indoor Settings		
9	Burgmann et al. [26].	Reduction of Aerosols through air purifiers in a classroom.
10	Narayanan et al. [27].	Effects of portable purifiers on virus laden aerosols inside a music classroom.
11	Abuhegazy et al. [28]	Aerosol transport and surface deposition in a classroom.
12	Foster et al. [29].	Compares infection risk of wells-riley model and CFD model
13	Yan et al. [30].	Infection risk in an airliner cabin using the wells-riley model
14	Liu et al. [31].	Risk analysis through aerosol transport in an air-conditioning restaurant.
15	Zhang et al. [32].	Covid transmission study through aerosols in an urban bus
16	Yang et al. [33].	Disease transmission for various R.H. and air-conditioning systems.
17	Yang et al. [34].	Effects of purifiers on covid transmission of droplets in a bus
18	Yao et al. [35].	Window opening effect and window position on aerosol transmission in a bus.
19	Komperda et al. [36].	SARS-COV-2 transmission in a large dental clinic
20	Li et al. [37].	Implemented, Particle velocimetry technique to analyse aerosol transmission in a dental clinic.
21	Mathai et al. [38].	Effect of ventilation and speed on aerosol transmission in a passenger cabin.
22	Vernez et al. [39].	Aerosol transmission in a poorly ventilated courtroom.
23	Cammarata et al. [40].	Dynamic evaluation of risk of viral infection in air

24	Venkatram et al. [41].	Implemented eddy diffusivity to model turbulent aerosol movement inside rooms.
25	Dbouk et al. [10].	Ventilation effect on aerosol transmission in enclosed spaces.
26	Sen et al. [7].	R.H., Ventilation Settings, Discharge direction and temperature effect on risk transmission.
27	Drivas et al. [42].	Developed an analytical model for assessing risk from short-term indoor contaminants.
28	Xie et al. [43].	Droplet travel distance in indoor settings.
29	Miller et al. [44]	Investigated super spreading event of skagit valley chorale.
30	Ai et al. [45].	Spread of expiratory droplet nuclei in an indoor environment.
31	Pal et al. [14].	Droplet dispersion in an indoor ambience.
32	Cheng et al. [46].	Trajectory of big respiratory droplets in R.H. in indoor environments.
33	Srinivasan et al. [47].	Viral load dependency of residence periods of virus-laden droplets from covid infected patients in indoor settings.

Wells-Riley Risk analysis Model		
34	Peng et al. [51].	Used improved wells-riley model for infection risk quantification
35	Guo et al. [52].	Assessed infection risk using wells-riley model and flow impact factor
36	Shao et al. [53].	Quantified infection risk using wells-riley model
Dose-Response Risk analysis Model		
37	Dhawan et al. [55].	Implemented stochastic dose-response model for infection risk quantification.

From the above discussion, we understand that an indoor domain poses a significantly higher risk of infection from virus-containing respiratory droplets as compared to an outdoor setting. Furthermore, the presence of poor ventilation in an indoor domain further confounds the issue. Hence investigation of an indoor enclosed domain is very essential. In agreement with this developed understanding, in this current study, an elevator domain commonly used in small enterprises or housing complexes has been chosen as the subject of investigation. Furthermore, such elevators are often poorly ventilated which also increases the infection probability. Hence, droplet transmission and evaporation has been rigorously studied in this work. However, there is a dearth of literature data on these aspects and hence has been addressed in this work. The outstanding issues has been enumerated below.

1.5. Outstanding Issues

- It is known that the virions are contained in the salt and protein-laden respiratory droplets. However, most numerical investigations have considered droplets to be made up of pure water, which does not portray a realistic scenario. Non-volatile salts in precise quantities are present in the droplets, and these salts encompass the virus. A respiratory droplet composed of a saline solution will have thermophysical properties that differ greatly from those of a droplet composed of pure water, and these thermophysical characteristics will alter as the water in the droplet evaporates. This variation and continuous evolution in thermophysical characteristics will result in a change in mass transfer number and hence mass loss rate through evaporation, resulting in a change in overall droplet dispersal as compared to pure water. The salt-laden droplets will finally convert into aerosol after evaporation of pure water (solvent). Quite a few studies done recently have revealed that the aerosol mode of virus transmission is supported by sufficient evidence[10,48,49]. Aerosols typically have a size lesser than 20 microns, allowing them to linger in the air for longer periods. Furthermore, based on current research, it may be argued that the aerosol contains the virions that cause disease transmission[50]. As a result, to resolve the issue discussed above and make simulations and their accompanying findings more

authentic, the present study has considered the respiratory droplets to be made up of water and salt in certain proportions[6]. The actual composition of a respiratory droplet varies significantly with factors like age, gender, and state of health of the emitting person. So, it is difficult to ascribe a unique set of properties to the droplets ejected by an infected person. However, it has been shown that a salt solution can act as a reasonable surrogate for respiratory droplets[14]. The difference in the evaporation and dispersion characteristics of the droplet of a dilute saline solution is within the range of variation exhibited by respiratory droplets from different sources[14].

- Several previous studies investigating the transmission risk associated with respiratory droplets in an enclosed domain have not undertaken a detailed epidemiological investigation. Biswas et al. tried to quantify the risk of infection based on the droplet count that might be inhaled by a susceptible person[50]. Sen has also followed a similar approach for risk quantification[7]. In reality, the risk of infection depends on the number of virions inhaled by a person and does not depend on droplet count only. For this reason, in this current study, for all formulations pertaining to the risk of infection, the virion counts supposedly inhaled by the susceptible person has been considered. Moreover, the majority of the studies that have taken into account the virion count have employed the classical Wells-Riley model for evaluation of the risk of infection associated with the virus-containing respiratory droplets[51–53]. However, there are some major drawbacks of the Wells-Riley model. Firstly, the Wells-Riley model is built upon a basic assumption that the indoor environment under consideration is a well-mixed room. Therefore, in situations (such as the situations in our present study) with ventilations that are either unable to render a well-mixed environment or have a directional nature, this assumption loses its validity[54]. Secondly, the Wells-Riley model requires the backward calculated quanta generation rate data[55]which is not available for any unfamiliar ventilation scenario. Thirdly, the Wells-Riley model, through the backward calculated quanta generation rate, incorporates many implicit

errors (like geometry, ventilation, infectious source strength) and hence the model cannot be accurately used in any generic situation[55]. Additionally, the dose-response model considers a threshold dose, only after inhaling which the infection can be initiated, whereas, in the Wells-Riley model, there is no such concept of a threshold quanta or a threshold dose. Liu et al. compared four risk assessment models namely the Exposure Risk Index, Intake Fraction, Improved Wells-Riley model, and the Dose-Response model, and concluded that the dose-response is the most accurate one[56]. A more authentic approach for evaluating the risk of infection is to employ the dose-response model since it is free of these errors that are inherently present in the Wells-Riley model. The dose-response model does not require the assumption of a well-mixed room and bases the infection risk calculation on the straightforward pathogen count. Furthermore, dose-response models can consider many of the external influencing factors explicitly (such as air-flow pattern, spatial distribution, and dispersion of pathogens) and hence incur fewer implicit errors[55]. Hence, in our current study, the stochastic dose-response model[55] is used in place of the Wells-Riley model owing to the above-mentioned drawbacks of the Wells-Riley model and the corresponding triumph of the dose-response model over these drawbacks, as discussed earlier.

- When droplets are contained inside a limited space, they evaporate, transforming into aerosol and allowing them to float in the air for prolonged periods of time. Additionally, small-sized droplets not only have the highest potential in getting deposited in the alveolar and bronchial region[57] but also, speed up the infection process as the escape time of the virions out of the droplet is directly proportional to the square of droplet size[58]. The ramifications of infection depend largely on what portion of the respiratory tract the pathogens are deposited. Infections in the alveolar and bronchial regions i.e., in the lower parts of the respiratory tracts or the lungs are more severe than that occurring in the Extrathoracic region[59]. Hence comprehensive scrutiny of these most precarious droplets, which have evaporated into

aerosols, and their locations are also made, thus leading to recognition of local hotspots within the elevator domain, which must be attempted to be avoided by other fellow passengers. Apart from a generic understanding of the overall Infection Risk, these above analyses enable us to estimate the severity of the infection and the swiftness of infection initiation and infection spread. Although the virions lose their viability with the loss of water from the respiratory droplets, the half-life of the virions being in orders of magnitude much greater[60] than the exposure time of the elevator, the loss of viability has not been taken into account.

- Whenever a person sneezes or coughs in small confined places, such as an elevator, the aerosol will stay in the enclosure either suspended in the domain or get deposited on surfaces or escape out. Hence, these droplets present a risk of infection to another person traveling in the elevator both through direct and indirect transmission routes[55]. The majority of studies assessing the infection risk from the respiratory droplets have only considered the airborne route of infection. Very few studies have attempted to investigate the threat posed by the indirect mode of transmission posed by fomites. Biswas et al.[50]. attempted to present the risk of possible infection through the fomite mode by reporting the droplet count that gets deposited on the surfaces of the elevator. However, they did not quantify the risk of infection through a proper formulation. In this present study, we have investigated the infection transmission through fomite mode as well and tried to quantify the risk associated with it based on the dose-responsive model.

- Droplet transmission routes in an enclosed domain affect the airborne risk of infection. The evaporation and heat transfer characteristics of the respiratory droplets affect the droplet trajectories significantly[50]. The ambient conditions play a major part in the evaporation and heat-transfer characteristics, and hence ultimately on infection risk through airborne routes for reasons as discussed earlier. Different ambient and climatic settings were explored, taking into account various ventilation

conditions quiescent, fan and exhaust ventilation. This is because the ventilation scenarios dictate the droplet transmission routes and as discussed transmission routes dictate infection risk.

1.6. Objective

To address the above discussed issues, in the present study, a 3-D simulation has been used to investigate dissemination of respiratory droplets across an elevator and its evaporation as well as the risk it poses.

- Inside the elevator, there is an infected passenger who is coughing and injecting droplets into the domain. The droplets are considered to be composed of a saline solution containing 1% NaCl (salt) and 99% H_2O by wt. Computational Fluid Dynamics (CFD) approach using an Eulerian-Lagrangian framework, utilizing opensource software OpenFOAM has been employed to simulate the above situation.

- The Risk of Infection is quantified by a parameter called Risk Factor, whose formulation is based on the stochastic Dose-Responsive model. The spatial variation of the Risk Factor, as well as the average Risk Factor in the domain, has been enumerated for various climatic conditions and ventilation scenarios, seeking the most conducive condition which suppresses the Infection Risk significantly.

- Because of the differential infection severity due to pathogen deposition at various depths of the respiratory tract, the deposition potential of aerosolized droplets across various depths of the respiratory tract, particularly the Extrathoracic, Alveolar, and Bronchial regions, has been intensively investigated. Since, besides the airborne mode of infection, the fomite mode also presents a significant pathway for disease transmission, this mode of infection has also been investigated based on a rigorous formulation.

The following section provides a outline and a brief description of the chapters in this thesis.

1.7. Outline

- **Introduction:** This chapter describes the motivation as a mechanical engineer in contributing towards investigation of covid transmission through dispersal of respiratory droplets. This chapter also concludes from existing literature data that an indoor domain poses more infection risk as compared to an outdoor setting besides discussing the outstanding issues associated with the existing studies on transmission of virus containing respiratory droplets.

- **Respiratory droplet transmission inside the elevator :** In this chapter the droplet transport across the elevator for various ventilation and climatic ambiences has been investigated. The quiescent, Fan and Exhaust Fan has been investigated as the ventilation conditions. The effect of varied climatic ambience ranging from cold humid(15^0C, 70% R.H.) to hot dry (30^0C, 30% R.H.) to hot humid (30^0C, 70% R.H.) on droplet dispersion and heat transfer, has been investigated for each of the ventilation scenarios. This chapters also discusses in detail the mathematical and numerical modelling implemented in this study.

- **Epidemiological implications of droplet transmission:** This chapter focuses on the infection risk associated with each of the climatic ambiences for various ventilation scenarios. The formulation of infection risk is based on the dose response model. A detailed analysis of the spatial variation of risk across the domain has been represented and apposite solution has been prescribed to ensure minimum risk.

Chapter 2

Respiratory droplet transmission inside the elevator

In this chapter the droplet dynamics and heat transfer of the ejected respiratory droplets has been investigated for various ventilation and climatic ambiences has been investigated. The effect of varied climatic ambience ranging from cold humid(150C, 70% R.H.) to hot dry (30^0C, 30% R.H.) to hot humid (30^0C, 70% R.H.) on droplet dispersion and heat transfer, has been investigated for each of the ventilation scenarios.

2.1. Problem Formulation

I . Geometry

The computational domain consists of an elevator having a capacity of 5 persons which is portrayed in Fig. 4(a), describing its details. The dimension of the elevator is 1.2 X 1.2 X 2m, which represents a characteristic size of elevators present in housing complexes or small enterprises. Investigation of an elevator of relatively smaller size is incumbent as the risk associated with a smaller confined space is higher. At the top of the elevator, a circular mounting of 0.6 m diameter is provided. This top circular mounting is subjected to conditions specific to each particular scenario, as illustrated further in the Initial and Boundary Conditions section as well as in Table 2. This top mounting is a very important part as by altering the boundary conditions on this mounting, the various ventilation situations inside the elevator are realized. In the present study, boundary conditions representing a Fan or an exhaust fan at the top opening have been presented. The ventilation slots, 3% of the platform area, have been provided at the lower portion of the elevator side walls (complying with the European EN-81-1 code38). Instead of incorporating a human manikin, the features of the passenger namely, the head, face, mouth and remaining body parts have been represented with rectangular boxes, whose dimensions conform to that of an actual human being in an upright standing position, to reduce the complexity and the computational cost and time. Also, since our area of focus in the domain is far away from the passenger, implementation of a geometry that corresponds to an actual human being will have no effect on our desired zone

of interest. The passenger height is taken as 1.75m (the mouth height being 1.56 m) [39]. Figure 4(b) shows the isometric view of the passenger in the domain, which also shows the position of the passenger relative to the elevator walls. The mouth of the passenger, from which the cough droplets are injected, has been modelled as a rectangular-shaped aperture having a width of 40 mm and an aspect ratio of 8 [39], as shown in Fig. 4(c). Three ventilation different scenarios have been studied to comprehend the effect of air flow in the surrounding environment on transmission and evaporation of droplets, injected into the domain by coughing of the passenger. Droplets ejected in the domain due to the coughing of the passenger would traverse the domain, their trajectory being contingent upon the preponderant velocity field. Certain number of droplets could turn into aerosols based on the prevalent temperature and humidity. A number of droplets might escape, a few of them may stick on the various surfaces within the elevator, while the remaining ones will remain suspended in the domain for extended periods – the last ones being of major concern to us.

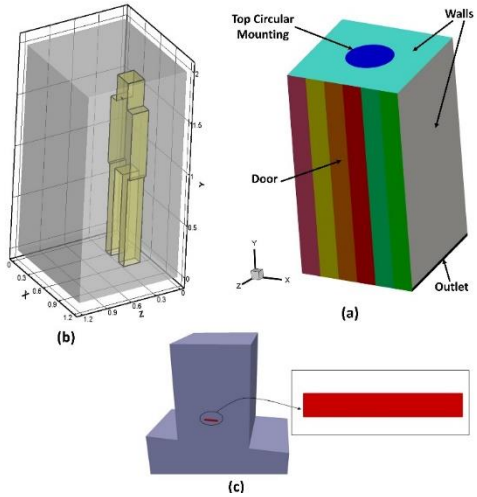

Figure 4: (a) The whole computational domain.
(b) Isometric view of the passenger in the domain.
(c) Mouth of the passenger modelled as a rectangular aperture.

II. Grid Independence Study

A 3D structured hexahedral-dominant mesh is used for the discretization of our computational domain. The mesh consists of approximately 5.8×10^5 cells. Mesh refinement is applied near the top mounting, outlets as well as other boundaries, but most importantly, sufficient refinement is applied near the passenger's mouth, from which the cough droplets are injected, to capture the droplet motion accurately. A smooth and gradual transition was also made from the very refined mesh near the mouth to the ambient mesh. A thorough grid independence study was conducted before selecting the above mesh. Three different mesh sizes; coarse (4,54,327 cells), medium (5,78,669 cells), and fine (6,95,027 cells) have been taken. The normalized eulerian field velocity V_y /V_{inlet} in a hot dry ambience having the top mounting implemented as an axial inlet jet ventilation condition (V_{inlet} = 0.56 m/s), is taken as the parameter, against which the results of the 3 different mesh are compared in Fig. 5 (b). The normalized axial velocity (V_y) profile is taken along a line AB of 0.6 m length, the line AB being parallel to the X-axis. The line AB is situated on the plane CD. The plane CD is parallel to the elevator's floor and is at a height of 1 m above the elevator floor. The line AB and the plane CD and their positions inside the elevator domain are shown in Fig. 5 (a). Besides the normalized axial velocity (V_y) profile, the velocity magnitude contours on plane CD are also compared in Fig. 5 (c). The spatio-temporal averaged risk factors are compared in Fig. 6. It can be seen that the results of the coarse mesh vary considerably from that of the medium and fine mesh and that the results of the medium and fine mesh have negligible difference. Since results become virtually grid independent with the medium and fine meshes, we adopted the medium mesh for our study. From this, it can be concluded that the medium mesh size considered here is adequate enough to capture the flow field correctly inside the elevator. Figures 7 (a) and 7 (b) show our finally adopted 3D mesh of 5,78,669 cells encapsulating the refinement near the boundaries and edges. Figure 7 (c) is showing a section of this mesh which portrays the gradual refinement near the mouth.

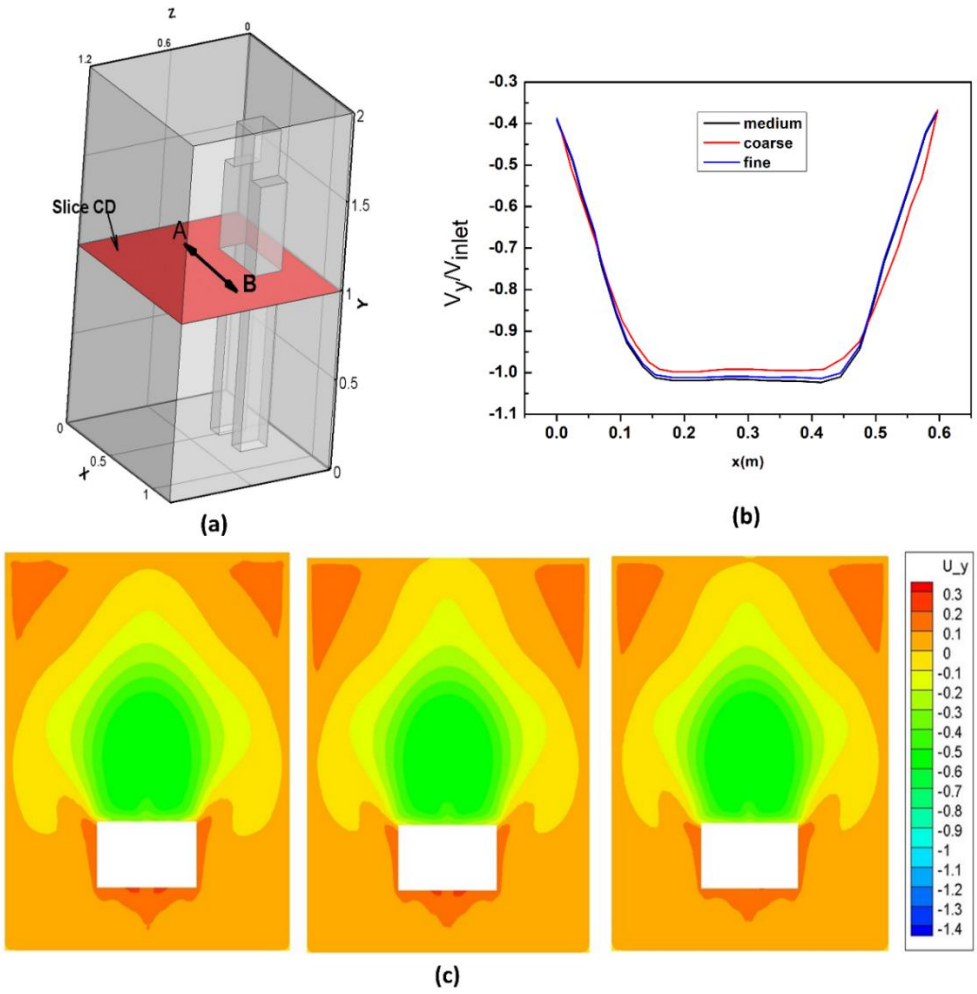

Figure 5: (a) Location of slice CD and line AB

(b) Comparison of Velocity profile(V_y) of different mesh sizes at line AB.

(c) Comparison of velocity contours of different mesh sizes at slice CD for coarse, medium and fine mesh sizes respectively from left to right

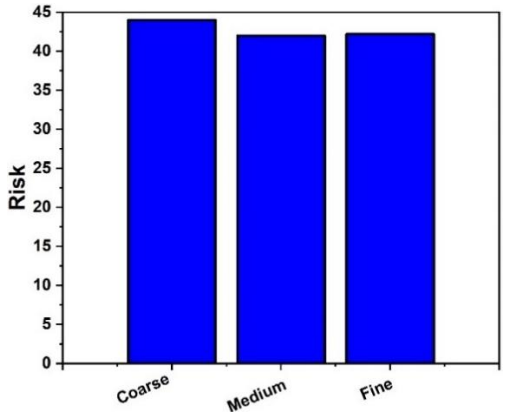

Figure 6: Comparison of the spatio-temporally averaged risk of infection of different mesh sizes (multimedia view).

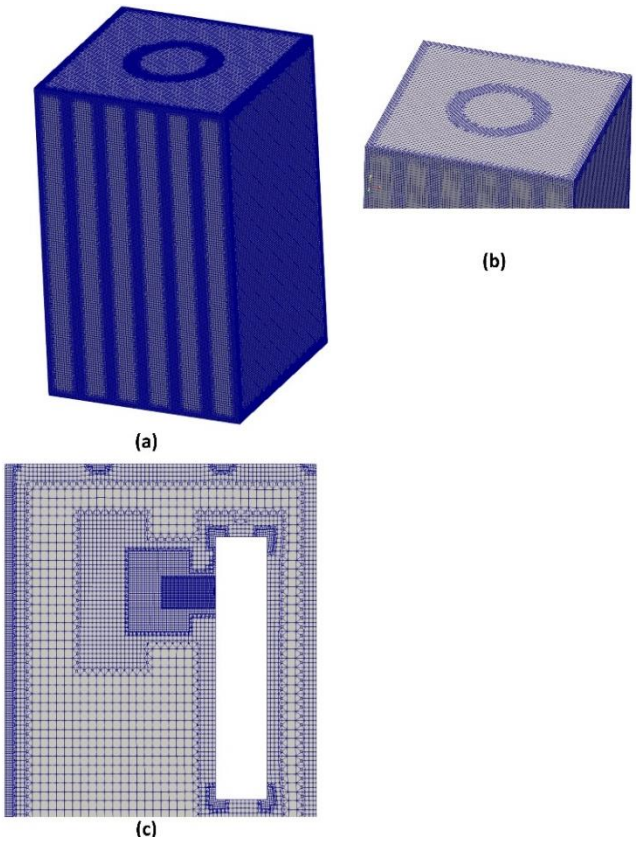

Figure 7: (a) Adopted Mesh

(b) Refinements at various locations of the adopted mesh

(c) Mesh Section showing gradual refinement of mesh near mouth of the Passenger

III . Mathematical Model

An Eulerian-Lagrangian model has been implemented for this numerical study. Air, the carrier fluid is modelled in the Eulerian frame. For the carrier bulk multiphase fluid mixture, the continuity (equation 1)[7,9] and the compressible multiphase mixture Reynolds-averaged Navier–Stokes equations (equation 2)[7,9] in conjunction with the k – ω turbulence model in the shear-stress-transport formulation (SST) (equations 3-15)[61] has been employed. Droplets that are injected into the domain due to coughing are treated as discrete particles and are solved in the Lagrangian frame of reference. The droplets roam around depending on the prevailing air velocity field and undergo evaporation as they traverse the domain. The droplets and moist air at the time of ejection from the mouth can be considered to be at the same temperature as that of the body temperature. Eventually, however the cloud of droplets intermingles with the surrounding air and it draws in a substantial amount of the surrounding ambient air following which the temperature of the cloud would effectually be identical to the surrounding ambient temperature [50] . But the evaporation process still continues (until the droplet becomes devoid of the volatile component), and the energy required for the phase change to happen is attained from the droplet and the surroundings (equation 22)[7]. The driving potential for the occurrence of evaporation of water is the difference of partial pressure of water vapour at the droplet surface and in the air encompassing the droplets (equation 27)[7]. The rate of evaporation depends upon the mass transfer coefficient determined from the Sherwood number (equation 28). Sherwood number, again, is dependent upon the droplet Reynolds number (equation 29)[9] based on the Ranz-Marshall correlation (equation 28)[48,62]. The droplet is considered to be a mixture of salt and liquid water (99% water and 1% NaCl by wt.). As the droplets evaporate to lose the volatile liquid mass into the ambient (equation 18)[7] and their diameter decreases, the mass fraction of its components changes (equations 32, 33) and finally the droplet fully evaporates i.e., becomes fully devoid of the volatile liquid water component, forming droplet nuclei. The droplet properties used in the

governing equations are a function of the properties of liquid water and salt as well as their respective mass fractions (equations 34, 35). The continuous change in the mass fractions of the components owing to the evaporation of the droplets has been taken into account (equations 31-33). Hence, to incorporate this salt model of the droplets (equations 31-36), modifications has been made in the source code of the reactingParcelFoam solver of OpenFOAM. The Ranz-Marshall model has been implemented to calculate the Nusselt number (equation 24) and Sherwood number (equation 28)[63,64], to solve the droplet heat transfer (equation 22) and mass transfer (equation 27)[7]. The droplet temperature is obtained by solving the energy conservation equation, as discussed below (equation 22)[7]. The evaporative cooling is modelled by taking into account the energy transfer from the bulk phase into Lagrangian phase (equations 15-17,23-24)[7]. The position and the velocity of the droplets are obtained by applying Newton's second law of motion on the droplets and the forces considered here are gravity, buoyancy, lift and drag (equations 21,25, 26)[7,9]. The relevant gas phase and particle phase transport equations with appropriate closure relations are given below.

Governing Equations for the Eulerian (Gas) Phase: -

Continuity equation

$$\frac{\partial \rho}{\partial t} + \frac{\partial}{\partial x_j}\left(\rho u_j\right) = m_v''' \qquad (1)$$

Momentum equation

$$\rho \frac{\partial u_i}{\partial t} + \frac{\partial}{\partial x_j}\left(\rho u_i u_j\right) = -\frac{\partial p}{\partial x_j} + \frac{\partial \tau_{ij}}{\partial x_i} + \rho g_i \qquad (2)$$

Closure equation for the momentum equation

$$\tau_{ij} = \mu_t \left(2S_{ij} - \frac{2}{3}\frac{\partial u_k}{\partial x_k}\delta_{ij}\right) - \frac{2}{3}\rho k \delta_{ij} \quad (3)$$

Strain rate

$$S_{ij} = \frac{1}{2}\left(\frac{\partial u_i}{\partial x_j} + \frac{\partial u_j}{\partial x_i}\right) \quad (4)$$

Transport equation for turbulent kinetic energy

$$\frac{\partial(\rho k)}{\partial t} + \frac{\partial(\rho u_j k)}{\partial x_j} = P - \beta^* \rho \omega k + \frac{\partial}{\partial x_j}\left[(\mu + \sigma_k \mu_t)\frac{\partial k}{\partial x_j}\right] \quad (5)$$

Transport equation for turbulent energy dissipation

$$\frac{\partial(\rho k)}{\partial t} + \frac{\partial(\rho u_j k)}{\partial x_j} = P - \beta^* \rho \omega k + \frac{\partial}{\partial x_j}\left[(\mu + \sigma_k \mu_t)\frac{\partial k}{\partial x_j}\right] \quad (6)$$

Turbulent kinetic energy production

$$P = \tau_{ij}\frac{\partial u_i}{\partial x_j} \quad (7)$$

Eddy viscosity limiter

$$\mu_t = \frac{\rho a_1 k}{\max(a_1 \omega, \Omega F_2)} \quad (8)$$

Weighted model constants

$$\phi = F_1 \phi_1 + (1 - F_1)\phi_2 \quad (9)$$

Blending function 1

$$F_1 = \tanh(arg_1^4) \quad (10)$$

Argument for blending function 1

$$arg_1 = \min\left[\max\left(\frac{\sqrt{k}}{\beta^* \omega d}, \frac{500\nu}{d^2 \omega}\right), \frac{4\rho\sigma_{\omega 2}\kappa}{CD_{k\omega} d^2}\right] \quad (11)$$

Blending function 2

$$F_2 = \tanh(arg_2^2) \tag{12}$$

Argument for blending function 2

$$arg_2 = \max\left(2\frac{\sqrt{k}}{\beta^*\omega d}, \frac{500\nu}{d^2\omega}\right) \tag{13}$$

Constants

$$\left.\begin{aligned}&\sigma_{k1} = 0.85, \sigma_{w1} = 0.65, \beta_1 = 0.075\\&\sigma_{k2} = 1.00, \sigma_{w2} = 0.856, \beta_2 = 0.0828\\&\beta^* = 0.09, a_1 = 0.31\end{aligned}\right\} \tag{14}$$

Energy transport from Lagrangian to Eulerian phase

$$\rho\frac{\partial H}{\partial t} + \frac{\partial}{\partial x_i}\left[\rho u_i H - \frac{\partial}{\partial x_i}\left(k_{eff}T\right)\right] = Q_d \tag{15}$$

Closure term for Energy equation

$$H = \sum x_i C_{pi} T_i \tag{16}$$

$$K_{eff} = k_{mol} + k_t \tag{17}$$

Species transport equation for water vapour

$$\frac{\partial(\rho f_v)}{\partial t} + \frac{\partial}{\partial x_i}\left[\rho u_i f_v - \rho D_{eff}\frac{\partial f_v}{\partial x_i}\right] = m_v''' \tag{18}$$

Closure term for the species transport equation

$$D_{eff} = D_{mol} + \frac{\nu_t}{Sc_t} \tag{19}$$

$$Sc_t = 0.7 \tag{20}$$

Governing Equations for the Lagrangian phase (droplet properties and parameters subscripted by d)

Equation of motion of droplet

$$m_d \frac{d\overrightarrow{u_d}}{dt} = \frac{\pi {d_d}^3}{6}(\rho_d - \rho)\vec{g} + \frac{C_d \rho \pi {d_d}^2}{8}|\overrightarrow{u_d} - \vec{u}|(\overrightarrow{u_d} - \vec{u}) + \overrightarrow{F_{lift}} \quad (21)$$

Energy-conservation equation, droplet phase

$$m_d C_{p,d} \frac{dT_d}{dt} = h\pi d_d^2 (T - T_d) + \frac{dm_d}{dt} h_{fg} \quad (22)$$

Energy transport from Lagrangian to Eulerian phase

$$Q_d = \frac{\sum_{i=1}^{i=N} \left(\pi d_{d,i}^2 h\left(T - T_{d,i}\right)\right)}{V_{cell}} \quad (23)$$

Ranz-Marshall correlation for Nusselt number

$$Nu = \frac{h d_d}{k_t} = 2.0 + 0.6 Re_d^{0.5} Pr^{0.33}, \; Pr = \frac{\mu}{\rho \alpha} \quad (24)$$

Drag coefficient

$$C_d = \max\left\{\frac{24}{Re_d}(1 + 0.15 Re_d^{0.687}); 0.44\right\} \quad (25)$$

Lift force

$$F_{lift} = \frac{2Kv^{0.5}\rho d_{ij}}{\rho_d d_d (d_{ik} d_{kl})^{0.25}}(\vec{u} - \overrightarrow{u_d}) \quad (26)$$

Droplet evaporation term

$$\frac{dm_d}{dt} = \pi d_d^2 m_{wl} k_{mt} \left(\frac{p_{sat}}{RT_d} - X\frac{p}{RT}\right) \quad (27)$$

Ranz-Marshall correlation for Sherwood number

$$Sh = \frac{k_{mt} d_d}{D} = 2.0 + 0.6 Re_d^{0.5} Sc^{0.33} \quad (28)$$

Droplet Reynold number

$$Re_d = \frac{d_d \rho |\overrightarrow{u_d} - \vec{u}|}{\mu} \quad (29)$$

Schmidt number

$$Sc = \frac{\mu}{\rho D} \quad (30)$$

Mass of nonvolatile component

$$m_d^s = Y_0^s m_d^0 \quad (31)$$

Mass fraction of nonvolatile component

$$m_d^s = Y_0^s m_d^0 \quad (32)$$

Mass fraction of volatile component

$$Y_d^l = 1 - Y_d^s \quad (33)$$

Droplet density

$$\rho_d = \frac{1}{\left(\frac{Y_d^s}{\rho^s}\right) + \left(\frac{Y_d^l}{\rho^l}\right)} \quad (34)$$

Droplet heat capacity

$$c_{p,d} = Y_d^s c_{p,s} + Y_d^l c_{p,l} \quad (35)$$

Droplet diameter

$$d_d = \left(\frac{6 m_d}{\pi \rho_d}\right)^{1/3} \quad (36)$$

IV. Initial and Boundary Conditions

The top circular mounting is assigned different conditions corresponding to three different scenarios i.e. quiescent, Fan and exhaust fan . Table 2 provided below elucidates this further. The two outlets provided at the lower portion of

the side walls are defined as pressure outlets with atmospheric pressure. All the walls and the boundary of the passenger are treated as walls with no slip velocity boundary condition. The door remains closed in all the scenarios and hence in all these scenarios, the door is modelled as a wall. By conducting numerical simulations, it has been inferred that the initiation time of the cough and air flow development in the domain has significant impact on the droplet kinematics. To eliminate this above stated bias and to make the situation more representative and generic, the cough is ejected in stages. The complete coughing phenomenon occurs in four stages. As depicted in Fig. 8, the coughing phenomenon commences at 1s and terminates at 4.12s. Each single cough occurs for 0.12s, injecting 1008 droplets of mass 7.7 mg with a velocity of 8.5 m/s normal to the mouth surface[7]. In each stream, the initial size distribution of the cough droplets follows the well-known Rosin-Rammler distribution or the Weibull distribution with a scale factor of 80 μm and shape factor of 8 [7] The passenger, assumed to be a symptomatic COVID infected patient, has a comparatively higher body temperature of 38.4℃. The continuous periodic inhalation and exhalation of the passenger has also been taken into account. The ambient pressure inside the elevator is one atmospheric pressure, 101325 Pa. The elevator is subjected to two different ambiences, 30℃, 50% R.H. (Hot dry) and 10℃, 90% R.H. (Cold humid). The temperature of the air ejected out of the mouth during exhalation is assumed to be at the body temperature and its relative humidity is assumed to be 100%[7]. The injected cough droplets are also at the body temperature. The cough droplets are considered as a mixture of NaCl (salt) and water with initial mass fractions of 0.01 NaCl (solid) and 0.99 water (liquid)[7].

IV. Numerical Method

The OpenFOAM solver “reactingParcelFoam”, with necessary modifications to successfully implement the salt model as discussed earlier was employed to solve all the required partial differential equations. It is very important to state that all the thermophysical properties of the Eulerian and Lagrangian phases are functions of temperature. The Eulerian phase has been modelled as an ideal gas for its equation of state, and its transport is modelled using Sutherland’s law[65] for its viscosity based on the kinetic theory of gases, which is suitable for non-

reacting gases. Finite volume methods have been employed to discretize the Eulerian phase. Second-order schemes have been employed for both space and time operators. Semi-implicit numerical schemes of second order have been employed for Lagrangian phase discretization.

Table 2: Table of Scenarios, *$\hat{\jmath}$ indicates positive y direction.			
Ambiences	Scenario	Objective	Angular Velocity of top circular mounting (rpm)[xx]
Hot dry (30℃,30% R.H.)	1	Effect of quiescent environment	0
	2	Effect of Exhaust Fan	$2000\hat{\jmath}$
	3	Effect of Fan	$-1100\hat{\jmath}$
Hot Dry (30℃,50% R.H.)	1	Effect of quiescent environment	0
	2	Effect of Exhaust Fan	$2000\hat{\jmath}$
	3	Effect of Fan	$-1100\hat{\jmath}$
Hot humid (30℃,70% R.H.)	1	Effect of quiescent environment	0
	2	Effect of Exhaust Fan	$2000\hat{\jmath}$
	3	Effect of Fan	$-1100\hat{\jmath}$
Cold humid (10℃,70% R.H.)	1	Effect of quiescent environment	0
	2	Effect of Exhaust Fan	$2000\hat{\jmath}$
	3	Effect of Fan	$-1100\hat{\jmath}$

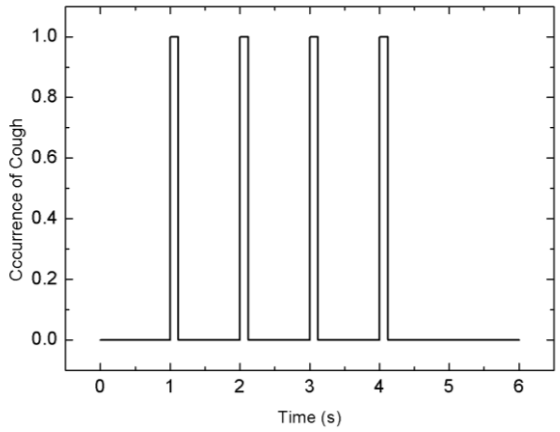

Figure 8: The entire coughing phenomenon

VI. Validation

A. Validation of Droplet Evaporation Model

Many previous studies have been conducted but the authors did not take into consideration the effect of soluble components present in the cough droplets. In

reality, cough droplets are not pure water and contain dissolved salts (like NaCl) in certain proportions. This presence of salts in cough droplets affects the droplet characteristics in several interconnected ways, as discussed in the Introduction section. In our study, an attempt is being made to make the simulations more realistic by considering the effect of salt solution in cough droplets i.e. by including the salt model of droplets. Our model is tested against the reported experimental result of change of diameter of an acoustically levitated 1 wt% salt (NaCl) laden droplet with time of Basu et al.[6].For this validation study, only 1 droplet (NaCl 1% by wt., H_2O 99% by wt.) is injected with initial size of 600 μm at the center of a domain. The quiescent condition is modelled appropriately by taking the domain size much larger than the droplet diameter and by assigning the internal field as well as the boundary fields of the entire computational domain a zero velocity. A temperature of 30℃ or 303K and a relative humidity of 50% is used as reported by Basu et al.[6]. In order to model the levitating droplet, the droplet is injected with zero initial velocity and no force (gravitational, buoyancy or sphere drag) is applied on the droplet, thus keeping it suspended in the domain indefinitely. The droplet diameter reduces continuously owing to its evaporation and the change in diameter (D) with time is noted. Figure 9(a) compares experimental data (Basu et al.[6]) of the temporal history of the instantaneous normalized droplet diameter (D/D_0; D_o initial diameter) with our numerically predicted results. The numerically predicted results are in a reasonably good agreement with the experimental observations of Basu et al.[6], as can be seen from the two graphs in Fig. 9(a). Hence our newly developed droplet salt model is validated.

B. CFD Model Validation

Before proceeding with the numerical model for our actual study, a quantitative validation of the droplet size distribution is done against the DNS data of size distribution reported by Ng et al.[66]. The validation data used are for temperature 30℃ and R.H. 90%, of Ng et al.[66]. For this validation study, the geometry and all the initial and boundary conditions are that of Ng et al.[66]. The droplet size distribution as predicted by our numerical (CFD) model is compared with the size distribution results of Ng et al.[66]. Figure 9(b) compares the droplet size distribution at t = 0.6s. The match between the droplet

size distributions is reasonably good. Thus, our numerical (CFD) model is validated and hence, our numerical (CFD) model along with our newly developed salt model can be used subsequently in our actual study.

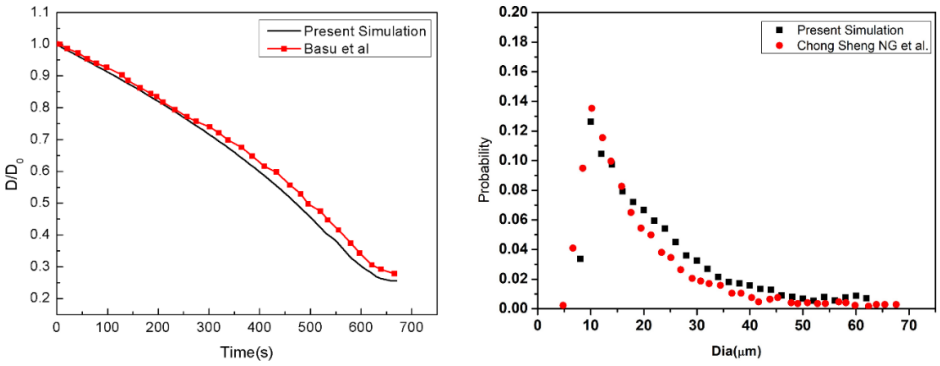

Figure 9: (a) Validation of droplet evaporation model including crystallisation with literature data[6]
(b) Validation of Droplet size distribution with literature data at t = 0.6s[66]

2.2 Transport and Evaporation droplets in various ventilation scenarios and climatic ambiences

2.2.1. Quiescent Scenario

In this scenario, the top mounting is treated as a wall, with no airflow interaction with the domain, thus making a quiescent environment prevail inside the elevator. For the hot dry cases, the droplets do not reach the floor within the stipulated elevator travel time of 10 seconds, as established by Fig. 10(a-b). It is important to note that droplets do not directly head towards the floor rather they get entrapped in the turbulence induced both by the cough and the continuous inhalation and exhalation of the passenger, and they get spread across the elevator. The absence of any continuous draft of air in the domain slows down the process of sticking or escaping of the droplets, hence majority of them remain suspended in the air. The suspended droplets evaporate continuously to decrease in size as visible from the continuous shrinking size

range, depicted by the diameter distribution of the suspended droplets at various time instances in Fig. 11(c-d). A probability distribution plot based on the initially injected droplet count has been used to represent the size distribution in Fig.11. Figure 11 also depicts the probability of droplet nuclei being formed. Droplet nuclei are the droplets from which the volatile liquid component has completely evaporated and is remaining only with the nonvolatile salt component. Due to the initial droplet size distribution following a Rosin-Rammler distribution, we have droplet nuclei of different sizes Fig. 11 and also it is possible to have a droplet and a droplet nuclei of same size Fig. 11. In this context, it is notable that out of a droplet and a droplet nucleus of same size, the droplet nuclei are more harmful as it has surely been inherited from an initially larger size droplet, thus exhibiting a very high viral load[50]. Furthermore, droplet in the size range less than 20 μm has the highest penetration ability in the lower parts of the respiratory tract namely the alveolar and bronchial regions which can lead to severe complications. Also, the droplet nuclei basically consist of only the non-volatile component, which in turn contains the pathogen. A significant number of suspended droplets evaporate to form droplet nuclei having size mostly in the range of 10-20 μm after 10s as shown in Fig. 11(c-d). Droplet nuclei are only found in the hot dry ambience and not in the cold humid ambience as in the later there is negligible evaporation thus preventing the formation of nuclei.

Contrasting results are obtained for the cold humid and hot humid ambience as shown in Fig. 10(c-d). as well as from the size distribution at various instants of elevator travel time as can been seen from Fig. 11(a-b). Due to their relatively larger mass as compared to the hot dry condition owing to negligible evaporation, the gravity force dominates over the injected droplets which ultimately cause the droplets to descend and reach the elevator within the stipulated time of 10s as can be seen in Fig 7(c-d). Moreover, the relatively larger diameter due to negligible evaporation, as compared to the hot dry condition produces a larger drag force on the droplets which prevents the spread of droplet in the elevator and produces an orderly downward motion. Although a few droplets are initially trapped in the turbulent puff of coughing and spread wayward, but owing to the gravity effect and larger drag force, they quickly

settle down. As can be observed from Fig. 11(d) for cold humid ambient, there is a slight increase in mean diameter initially, followed by a monotonic decrease. This can be explained by the phenomenon of supersaturation at high humidity, as reported by Chong et al.[66].

2.2.2. Exhaust Fan ventilation Scenario

In this scenario the top mounting is modelled as an exhaust fan. Here the fan rotates with a r.p.m of 2000 to suck air out of the domain. The flow develops quickly in the domain (especially near the man's mouth) to develop a sufficient strong drag force, for all the ambient conditions as depicted by the temperature contoured velocity vector plots in Fig. 13(in Plane AB, Fig. 12). Hence, the particles move upwards immediately upon injection due to the more enhanced drag force exerted by air on the particles, as can be seen from the droplet dispersion transience depicted in Fig. 14. The circulation brought about by the rotational effect, increases the dispersion in droplet kinematics due to the additional turbulence (created by the rotating component of the fan), due to which the droplets rise up and a significant amount of them gets deposited at the roof (top wall) of the elevator. As can be understood from the droplet distribution in Fig. 14 for the hot dry ambience, after 5.5 s, none of the droplets remain below the height of the passenger whereas for the cold humid ambience, the elevator becomes safe but it takes 7.48 s. The time taken by the hot humid ambience to become completely devoid of droplets is same as that of the cold humid ambience. The droplet dispersion for the exhaust fan scenario has been represented for the hot dry (30^0C, 30% R.H.) and cold humid (30^0C, 50% R.H.) ambience only since the remaining ambiences show similar trajectory i.e., within a certain interval the domain becomes completely safe. Hence the domain becomes completely safe from these time instants for both the ambient conditions. Since a negligible percentage of injected droplets remain suspended in the domain at all time instants, the size distribution has not been investigated.

Scenario	Hot, Dry (30^0C,30% R.H.) (a)	Hot, Dry (30^0C,50% R.H.) (b)	Hot, Humid (30^0C,70% R.H) (c)	Cold,Humid (15^0C,70% RH.) (d)
Time=4.14s	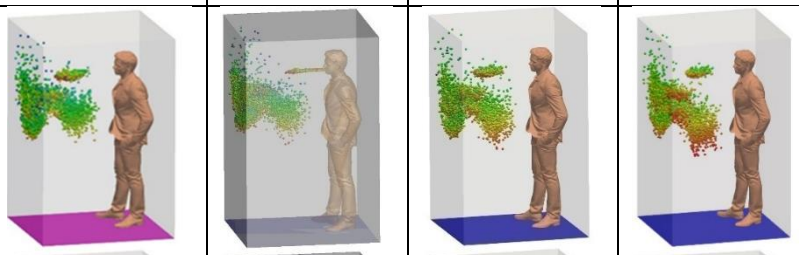			
Time=5.5s	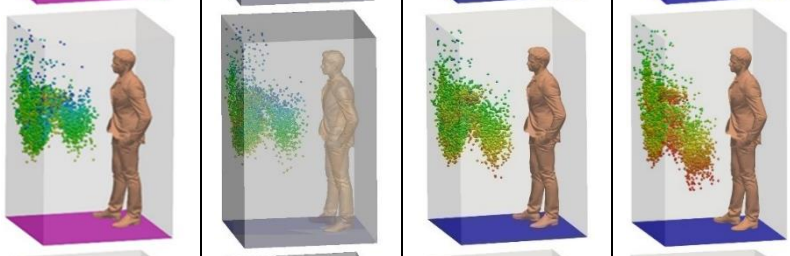			
Time=7.5s	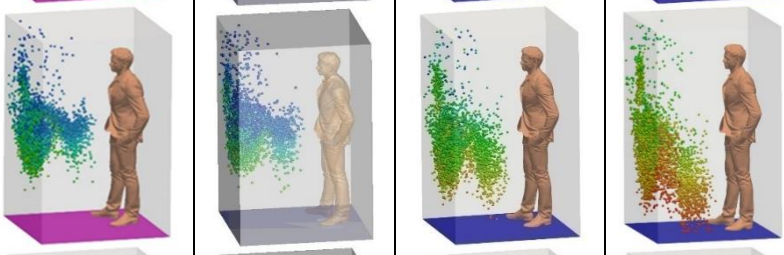			
Time=9s	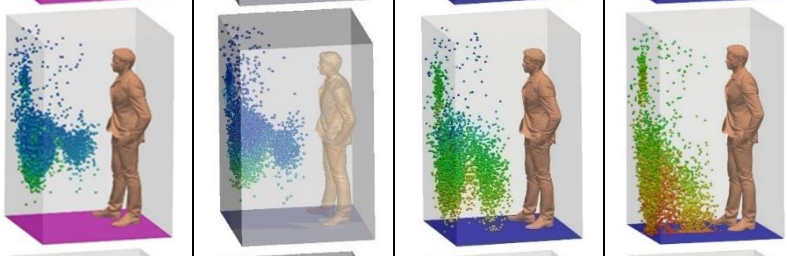			
Time=10s	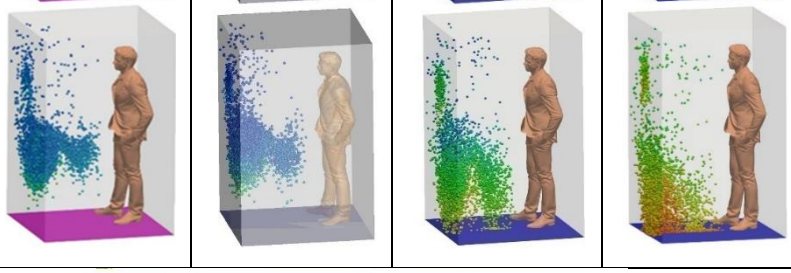			
				

Figure 10:(a)-(d) Droplet dispersion in the domain at various time instants for quiescent scenario of all the ambiences.

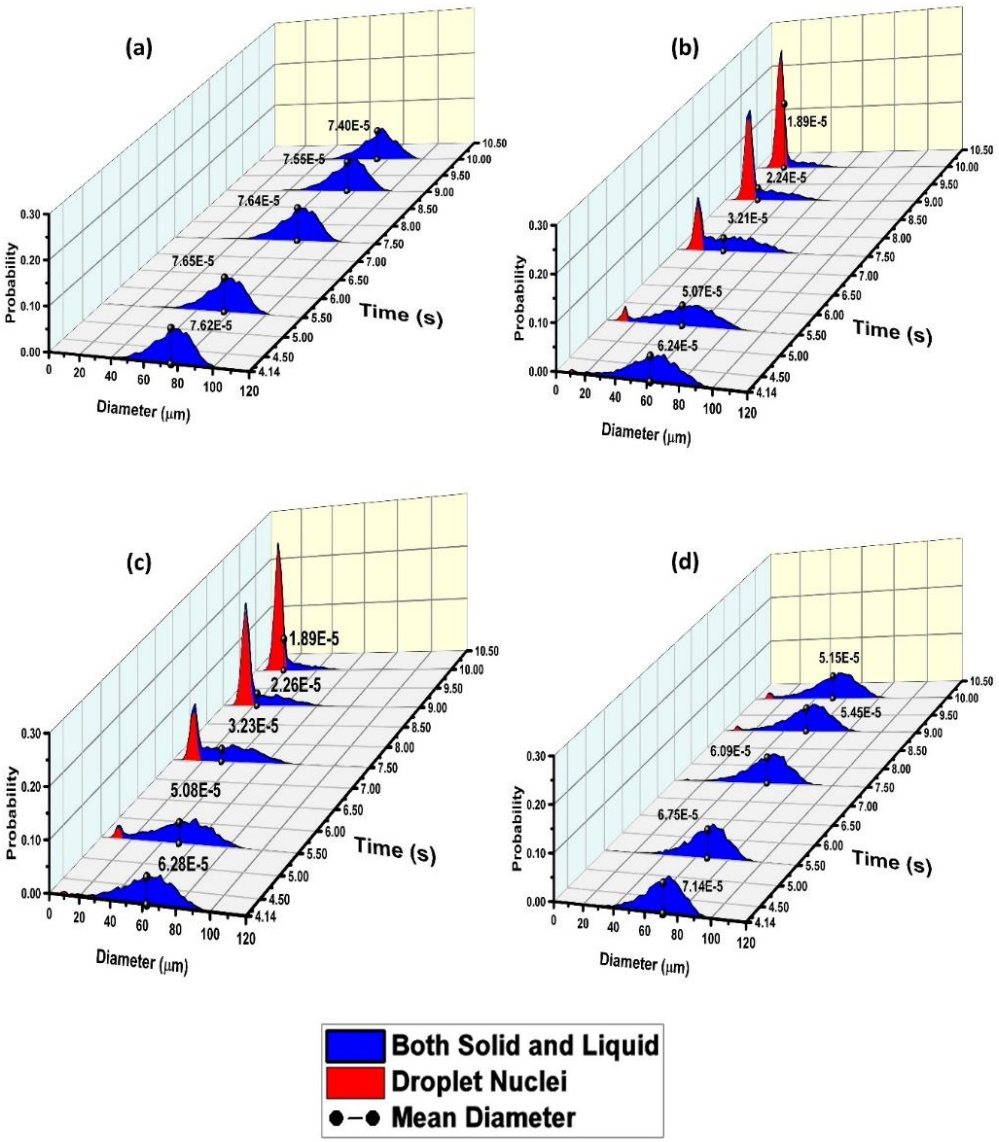

Figure 11:(a)-(d) Diameter size distribution of suspended droplets in the domain at various time instants for quiescent ventilation scenarios for cold humid (15^{o}C, 70% R.H.), hot dry (30^{o}C, 30% R.H.), hot dry (30^{o}C, 50% R.H.) and hot humid (30^{o}C, 70% R.H.) climatic ambiences respectively.

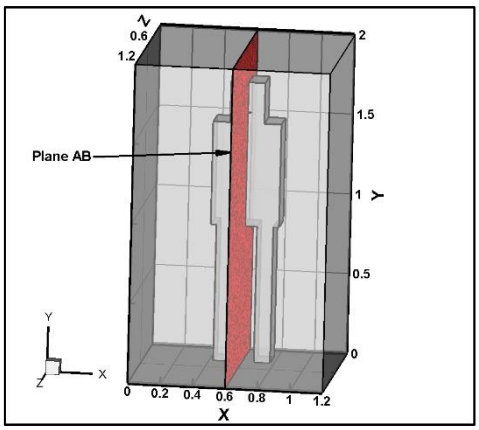

Figure 12: Showing cross-sectional plane AB .

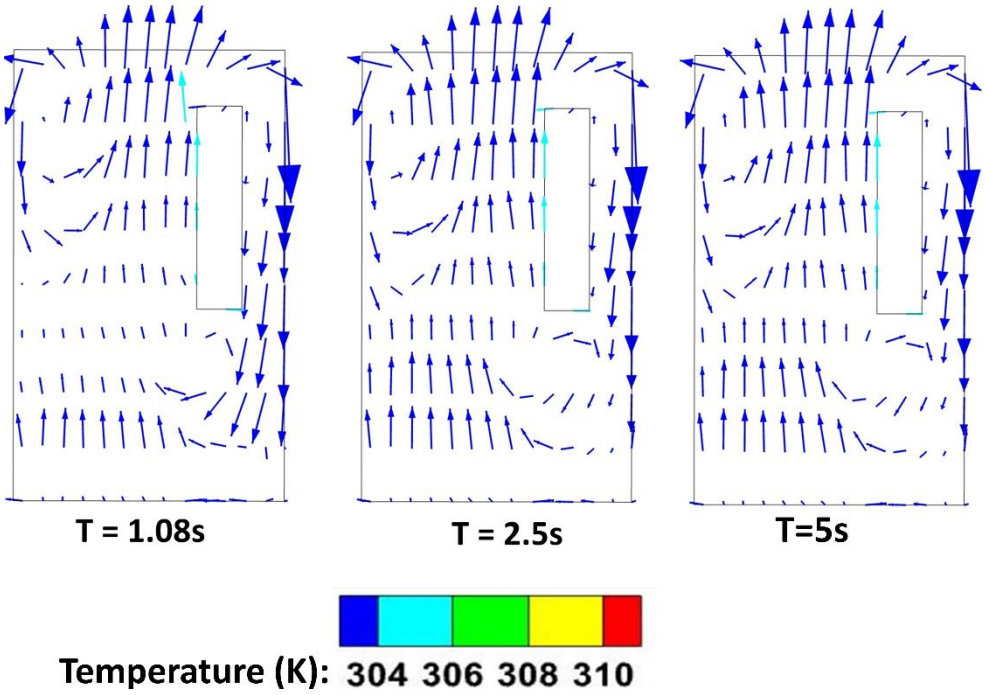

Figure 13: Temperature contoured velocity vector plots at plane AB (of Fig. 12) at different time instances, of exhaust ventilation for the hot dry ambience.

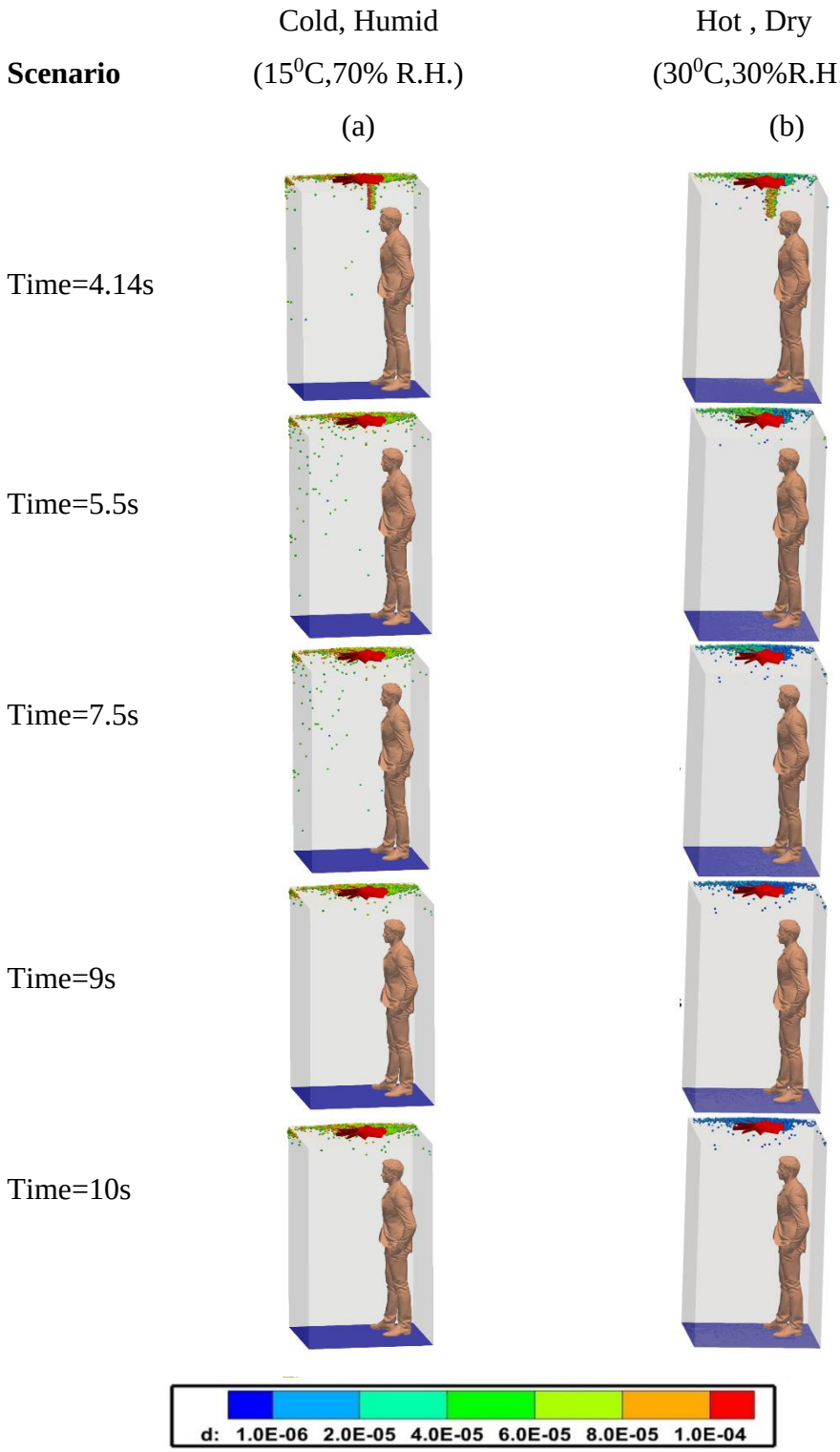

Figure 14:(a)-(b) Droplet dispersion in the domain at various time instants for exhaust fan scenario for cold humid and hot dry ambience.

2.2.3. Fan ventilation Scenario

We infer from the preceding discussion that the absence of forced convection in a domain is unfavourable for enclosed domains because droplets remain suspended in the domain for extended periods, resulting in a very high-risk situation. As a result, we attempted to investigate the influence of forced convection on droplet dispersion characteristics by modelling the elevator's top mounting as a Fan. Although it has been shown earlier that the exhaust fan completely mitigates the infection risk by causing all the droplets to escape very quickly , the exhaust ventilation scenario is not ubiquitous rather the Fan ventilation is. This is why the Fan ventilation scenario has been investigated to discern whether it can mitigate the infection risk.

The droplet dispersion in the domain is depicted for various Fan RPMs and volume flow-rates [67,68]in Fig. 15. One interesting aspect pertaining to the droplet dispersion that needs to be noted is that the droplets upon injection from the mouth initially go up and then descend down. The droplets upon being injected from the mouth get trapped in the vortices near the mouth and hence go up. The velocity vector plots (on plane AB, Fig 13(a)) in Fig 16 depict the vortices developed near the coughing passenger's mouth. As seen from Fig.16, there is a weak velocity field and weak vortex created at low RPM (500 RPM), whereas there is a strong velocity field and strong vortex formed due to the enhanced induced turbulence brought about by the increasing rotating component of the fan at high fan speed (1100 RPM). In quiescent case, the droplets descend down slowly (but steadily) and orderly. The weaker vortices of the low-speed fan keep the droplets levitated for a substantial amount of time whereas the strong vortices of the high-speed fan causes a significant percentage of droplets to stick on the domain walls. The droplet dispersion and its temporal history for various Fan speeds depicted in Fig. 15 bolsters this argument. The above argument establishes that there is a increase in infection probability (since quantity of airborne droplets increase) as we go from Quiescent to low RPM Fan and the decrease in infection probability as we go from Quiescent to high RPM Fan (since quantity of airborne droplets decrease significantly). A rigorous infection risk formulation based on the dose response model[55] has been done (explained in detail in the next chapter) and it was determined that

increasing the Fan RPM beyond 1100 does not decrease the infection risk significantly, hence 1100 RPM is chosen as the Fan speed which maintains a significantly low infection risk. In the fan ventilation scenario, circulation caused by the rotational effect enhances the droplet dissemination owing to increased motion (produced by the rotational component of the fan), causing dispersal of droplets to far-off locations and eventually get stuck at various elevator surfaces or fall below the inhalation breathing box height within a

Scenarios / Time	RPM 500(a)	RPM 700(b)	RPM 1000(c)	RPM 1100(d)
t=4.14s	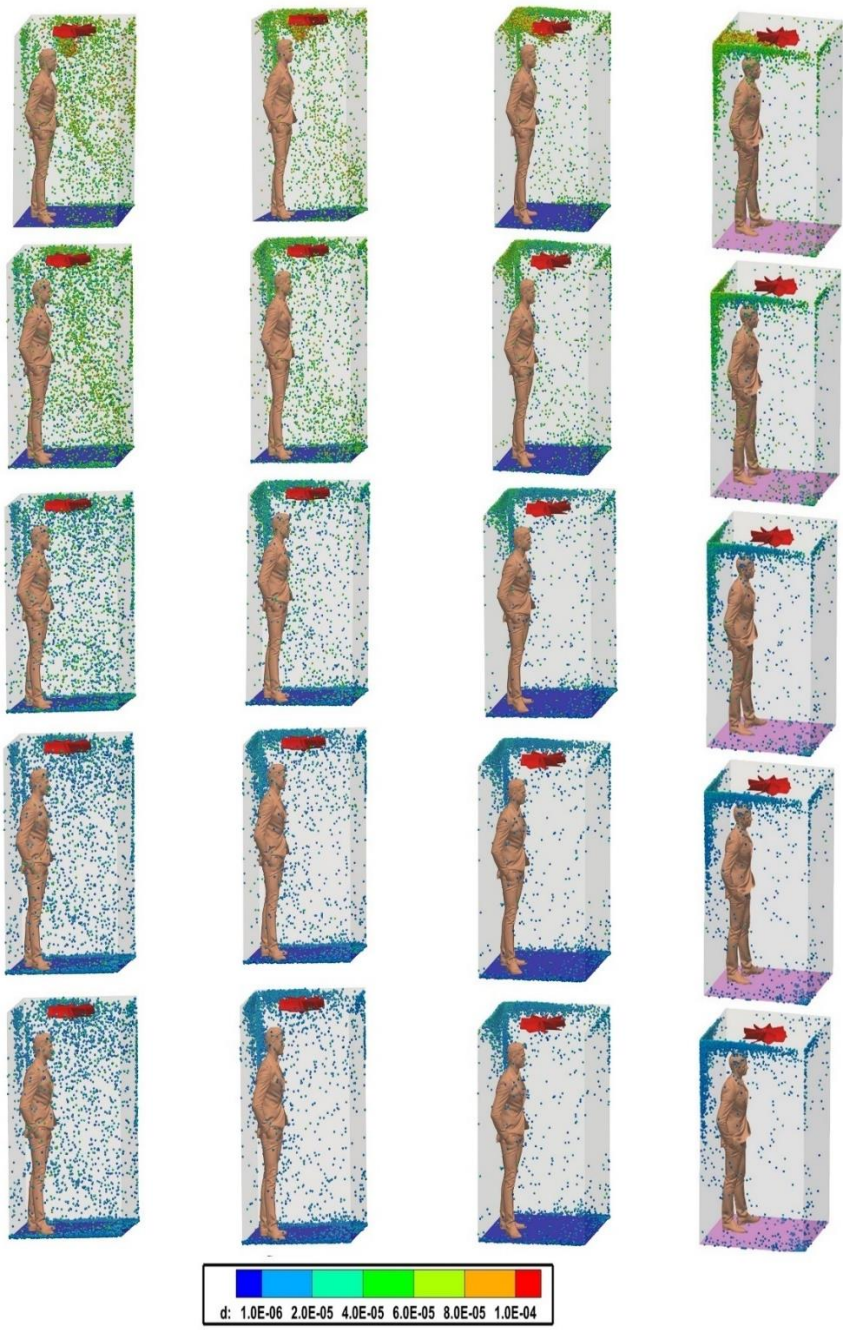			
t=5.5s				
t=7.5s				
t=9s				
t= 10s				

Figure 15 :(a)-(d) Droplet dispersion in the domain at various time instants for the Fan ventilation scenarios for hot dry ambience (30^0C, 50% R.H.), for fan speeds 500, 700, 1000, 1100 RPMs.

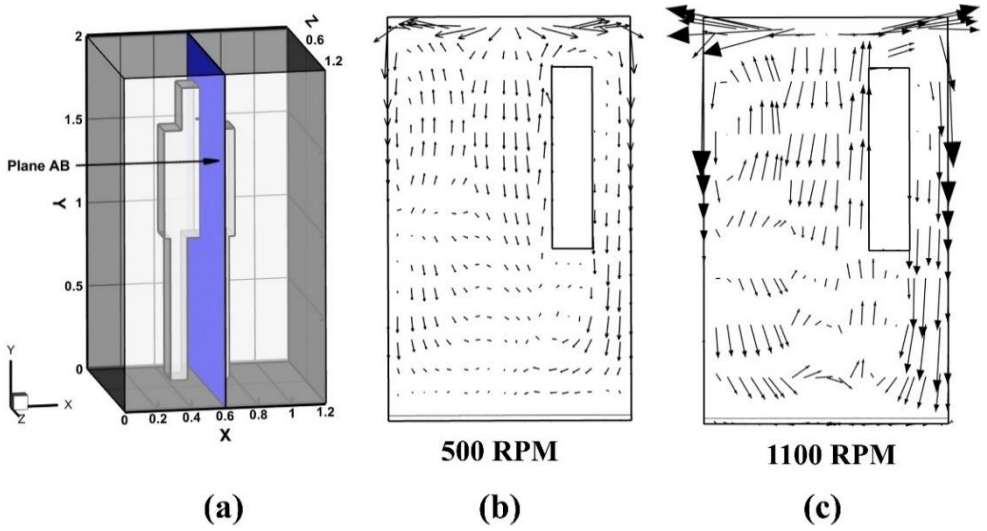

Figure 16 (a)-(c): Plots the velocity vectors for various Fan velocities on Plane AB(Fig. 16(a)) .

short span. The air-flow pattern brought about by the fan ventilation scenario at 1100 rpm outweighs major changes brought about by climatic influences on droplet dynamics. Hence climatic ambient conditions and their corresponding evaporation characteristics have less effect in dictating the droplet dispersion in the fan ventilation scenario as depicted in Fig. 18. For all climatic conditions, a fan speed of 1100 rpm is maintained. Figure 17 demonstrates the probability distributions of diameter of the lingering droplets for the fan ventilation scenario. It reconfirms the fact that a significantly less fraction of injected droplets lingers in the domain for the fan ventilation scenario. The diameter distributions demonstrate the effect of ambient conditions on droplet evaporation as indicated by the increase in droplet nuclei percentage with the change of ambient conditions from cold humid to hot dry. Although it has been concluded that climatic ambiance does not have a significant impact on the droplet dispersion in the fan ventilation scenario, Fig. 17 confirms that the fraction of suspended droplets in the hot dry ambience is greater than that of the cold-humid ambience owing to the difference in their evaporation characteristics as discussed above.

2.2.4. Effect of Door Opening

The introduction of forced circulation in the form of Fan and Exhaust Fan significantly reduces the fraction of suspended droplets in the domain, however that is not the scenario with quiescent domain where a significant quantity of droplets continue to linger. Droplets may continue to linger even after the infected person leaves the domain. Therefore it is important to discern what is the safe time after which the lift can be deemed to be safe for reuse , after the abeyance of the infected person. For, this study the door is opened, the passenger leaves the domain and the door is again closed. The time after the leaving of the person when the entire domain becomes devoid of droplets is determined. The opening of the door began at 4.25 seconds and continued till 5 seconds. The person leaves the domain at the end of 5 seconds. The door remains open till 6 seconds and again closed within 6.75 seconds. It is found that after this exercise, as elucidated in Table 3 no droplets remain in the domain and there remains no risk of infection as seen from Fig. 19. The opening and closing of the elevator was maintained following the ASME A 17.1 safety guidelines for Elevators and Escalators[69]. Thus, one can safely conclude that within the timespan of opening and closing of the elevator, 2.5 seconds, all the droplets leave the domain and the lift is completely safe to be used again.

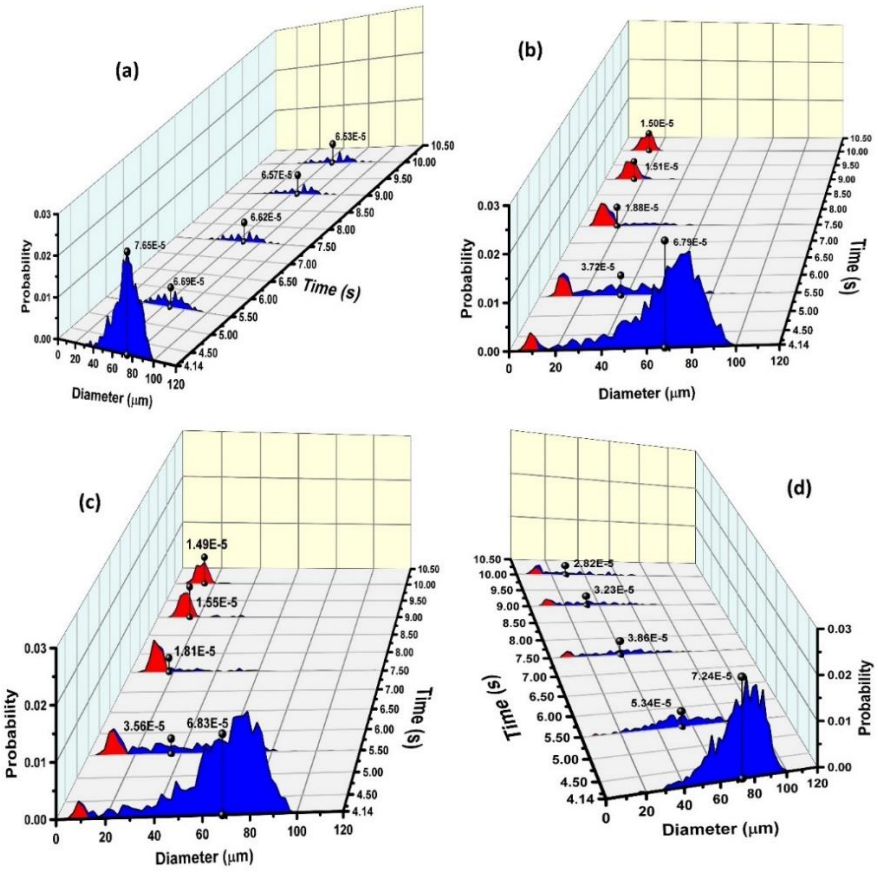

Figure 17:(a)-(d) Diameter size distribution in the domain at various time instants for Fan ventilation scenario (1100 RPM) for cold humid (15^{o}C, 70% R.H.), hot dry (30^{o}C, 30% R.H.), hot dry (30^{o}C, 50% R.H.) and hot humid (30^{o}C, 70% R.H.) climatic ambiences respectively.

Scenario	Hot, Dry (30^0C,30% R.H.) (a)	Hot, Dry (30^0C,50%R.H.) (b)	Hot, Humid (30^0C,70%R.H.) (c)	Cold, Humid (15^0C,70%R.H.) (d)
Time=4.14s				
Time=5.5s				
Time=7.5s				
Time=9s				
Time=10s				

Figure 18:(a)-(d) Droplet dispersion in the domain at various time instants for Fan ventilation scenario of all the ambiences.

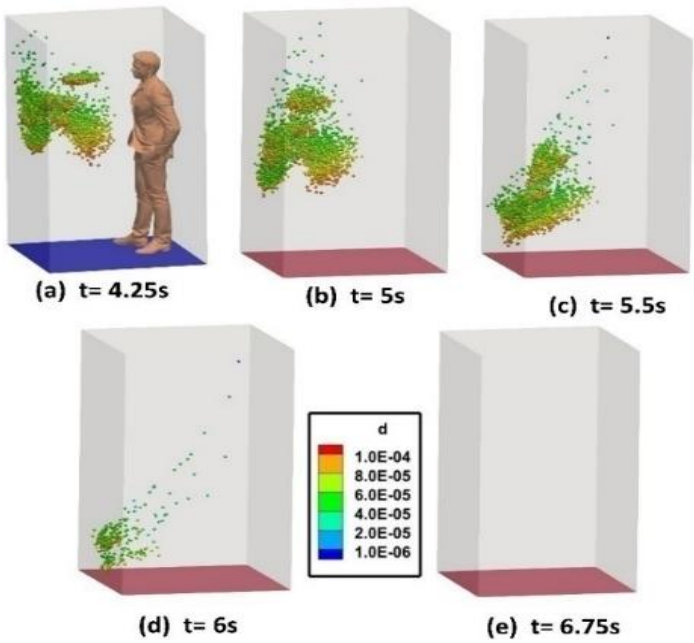

Figure 19:(a)-(e): Droplet dispersion in a quiescent domain for door opening scenario for hot dry climatic condition (30^0C, 30% R.H.) at 4.25s, 5s,5.5s,6s,6.75s respectively

Table 3: Enumerating the processes at different time instants	
Time	**Definition**
4.25s	Door Opening begins
5s	Door Opening completes, and Passenger leaves the domain
6s	Door Closing begins
6.75s	Door Closing complete.

2.3 Concluding Remarks

This chapter reports the droplet dissemination in various ventilation scenarios namely the quiescent, Fan and Exhaust Fan. In the quiescent scenario there is an orderly motion of the droplets. The hot dry climatic ambience causes the droplets to evaporate very quickly in the domain and hence, causes them to linger in the domain for extended period of time thus creating a high risk situation. The cold humid and hot humid ambience on the other due to the very negligible evaporation causes the heavier droplets to descend and touch the ground much faster as compared to hot dry ambience. The implementation of

a forced circulation in the domain in the form of Exhaust completely changes the droplet dynamics. All the droplets escape out of the domain very quickly thus rendering the domain very safe. Although exhaust Fan provides the perfect ventilation solution it is not common in elevators. Hence, the Fan ventilation scenarios has been investigated. It was found that at low RPM a significant percentage of droplets remains levitated however at high RPMs, RPM greater than 1100 RPM the quantity of suspended droplets decreases significantly thus reducing the infection risk possibility. Finally the safe time for elevator reuse after the infected person has left the domain is determined.

Chapter 3

Epidemiological implications of Droplet Transport

It has been established in the previous chapter that the droplets escape out of the domain very quickly in an Exhaust Fan ventilation scenario. However for the quiescent and Fan ventilation scenario the droplets continue to linger in the domain. Therefore it is pertinent that a quantitative formulation of the infection risk in these ventilation conditions is the need of the hour. A rigorous formulation of the risk based on a stochastic dose response model[55] has been conducted for these two ventilation scenarios in various ambiences. The results of these formulations have been reported in this chapter. The dose response model computes the infection risk based on the quantity of pathogen inhaled. Infection probability of a susceptible person depends upon the virion quantity inhaled or transferred to a mucous membrane. Upon the inhalation or transfer of a certain threshold quantity a susceptible person stands a chance of being infected. The infection probability depends upon the virion quantity with respect to the threshold intake by the person. The equations below 37-39 describe these in detail.

The domain has been sub-divided into 16 breathing boxes (each of size 0.3m x 0.4m x 0.3m) as illustrated in Fig. 20. The Risk of Infection(R) is calculated in all of these boxes using a dose-response model[55,70] as per equation 37 below.

$$R = 1 - \exp(-\sigma\mu) \qquad (37)$$

μ is the expected number of pathogens likely to be inhaled by a susceptible person over the exposure time of elevator travel (10s), given by equation 38.

$$\mu = \sum_{\beta} \int_0^1 \frac{P}{V} \frac{\int_0^{T_0} \frac{c\pi}{6} D_0^3 N \, dt}{T_0} dt \qquad (38)$$

where D_0 is the initial diameter of injected cough droplet; N is the mean viral load in the respiratory fluid of covid-19 infected persons (7 X 10^6 RNA copies/ ml)[71]. P is the pulmonary ventilation rate[72], V is the volume of the considered breathing box and β is the total number of inhalation cycles over the total exposure time (T_0), considering an inhalation period of 1s[50]. $\frac{P}{V}$ represents the probability of inhaling a droplet suspended within the breathing

box. The infectivity factor, "σ", is the inverse of the number of viruses capable of initiating an infection and is a direct indication of the infectious dosage[70]. Infectivity factor for SARS-COV-2 as reported by a recent study by Mikszewski et al.[73] has been used for the current work. The dose-response model as discussed earlier in chapter 1, is devoid of some of the limitations of the Wells-Riley model due to its consideration of the external factors like ventilation, geometry, air-flow pattern as well as the actual pathogen content.

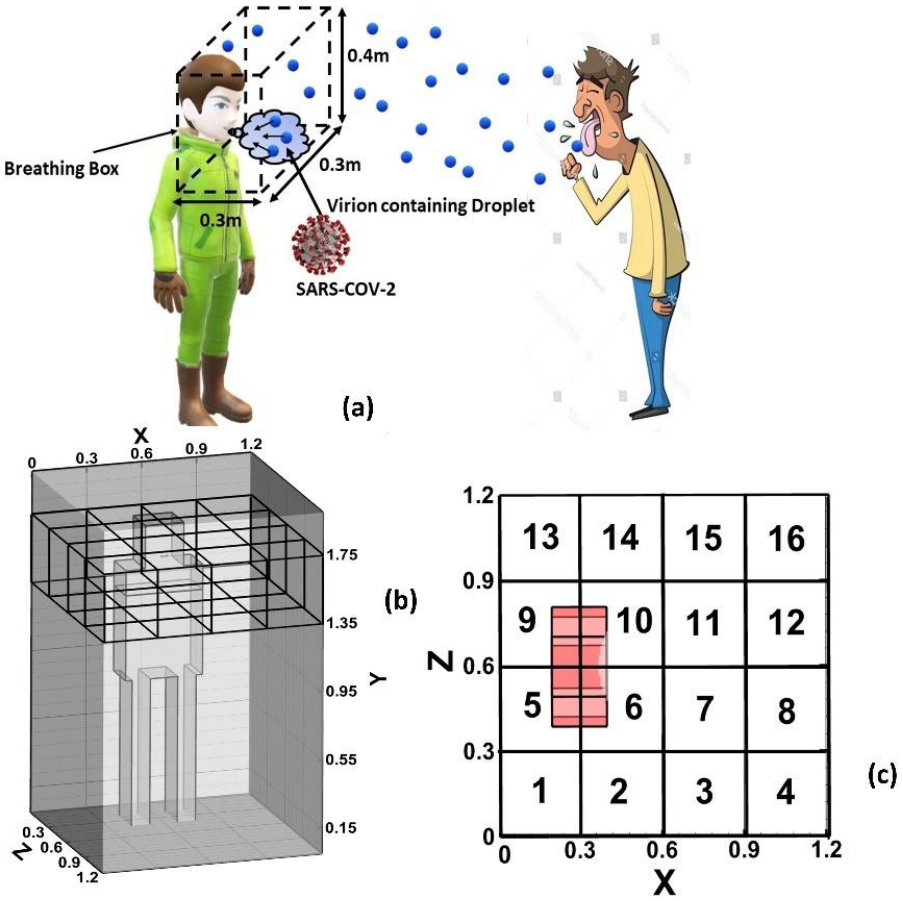

Figure 20: (a) Illustrative representation of a breathing box containing virion containing droplets and a susceptible person inhaling it.
(b) An isometric view of all the sixteen breathing boxes in the domain at a height of 1.35m
(c) Top view representing the passenger and location of all the sixteen breathing boxes with respect to the passenger.

3.1. Infection Risk in a Quiescent Scenario

Figure 21(c) shows the magnitude of risk of infection and its spatial variation over all the 16 breathing boxes of the domain for a quiescent hot dry scenario (30^oC, 30% R.H.). It depicts that in a quiescent scenario over the exposure time of elevator travel, a substantial portion of the elevator domain presents a significant risk of infection. The calculated spatial-averaged risk factor for the hot dry ambience (Spatial-averaged risk factor is the risk of infection(R), spatially-averaged over all the 16 breathing boxes) of 35.68% demonstrates that the quiescent scenario creates a high-risk condition inside the elevator. Furthermore, the hot and dry ambient environment leads to significant evaporation of the droplets leading to the development of a significant number of droplets in the size range of 5-20 μm. The droplets in this size range, virusols (droplet size<20μm)[74], derived from the relatively larger droplets have very high viral loads, less diffusion time of virions, and as discussed earlier due to their size being less than 20 μm have the highest potential for infection. In case of Quiescent ventilation scenario, the Risk is concentrated mainly in the region in front of the coughing person. This is because in case of Quiescent ventilation scenario, due to absence of any influencing airflow, the ensuing motion of droplets is ordered. The droplets move forward by virtue of their injection velocity from mouth, and descend slowly downward owing to gravity. Some droplets (being entrained in the turbulence generated by the cough and the constant inhalation and exhalation of the passenger) spread across the elevator, mainly towards the front right and left corners. Broadly speaking, in a generic Quiescent scenario, the region in front of the mouth of the infected coughing person (i.e. the four breathing boxes in front) present an immense Risk of infection for all the climatic conditions, as shown by Fig. 21(a-d). As concerning the front left and right corners, the behaviour is different among different climatic conditions. In the dry climatic condition cases, due to more evaporation, the droplets which make their way to these spots remain suspended there for extended periods, whereas for humid cases, the droplets albeit reaching these spots, fall off the breathing box height quickly, thus explaining the difference. This difference in evaporation characteristics brings about the

difference in droplet trajectories and ultimately the infection risk as depicted in Fig. 22.

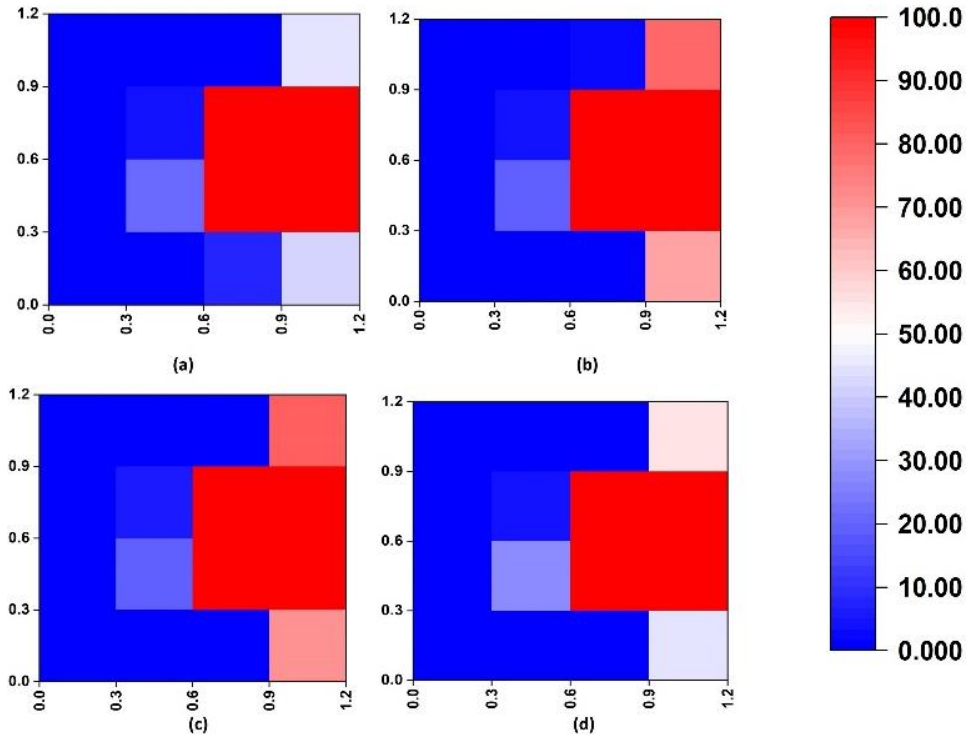

Figure 21 (a)-(d): Heat map showing the variation of risk of infection across the breathing boxes for quiescent ventilation scenario throughout the domain over the total exposure time for cold humid (15^{o}C,70% R.H.), hot dry (30^{o}C,30% R.H.), hot dry (30^{o}C,50% R.H.), hot humid (30^{o}C,70% R.H.) respectively

Until now, we have conclusively established that changes in climatic environments have a major impact on droplet transmission routes and ultimately on the risk of infection in a quiescent scenario. It is worth emphasising, however, that humidity is the more essential climatic aspect than temperature. Fig 23, depicts the spatio-averaged risk of infection over the total exposure time as the climatic settings from cold humid (15°C, 70% R.H) to hot dry(30°C, 30% R.H) to hot humid(30°C, 70% R.H).Keeping the temperature (30°C) same a change of 10.84% in average Risk Factor is observed with the change in humidity (30% to 70% R.H.) whereas a change of 1.2% is observed with the

change in temperature (30℃ to 15℃) at same humidity level (70% R.H.). Thus we conclude for per unit percent change in temperature a 2.4% change in risk of infection is observed whereas for per unit percent change in humidity the change in risk of infection is 19.29%. This emphasizes the fact that out of temperature and humidity, humidity is the more important climatic condition.

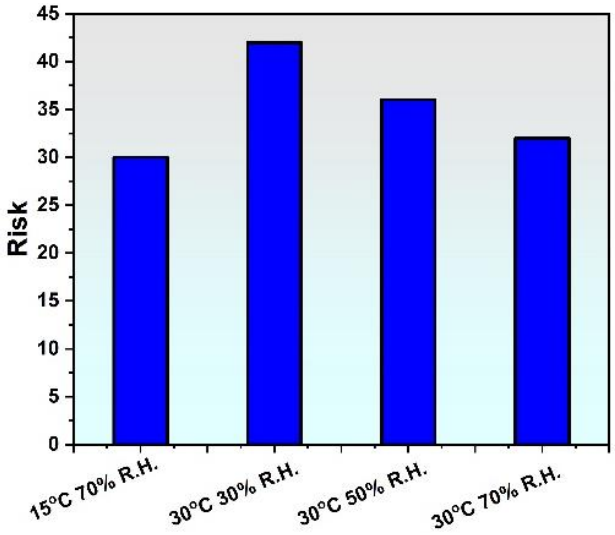

Figure 22: Showing the variation of spatio-averaged risk over the domain for various climatic ambiences for quiescent ventilation scenario.

3.2. Infection Risk in a Fan ventilation Scenario

The Fan ventilation Scenario has been sought to reduce the infection risk and the proper Fan RPM that needs to be maintained is determined. It has been established earlier at low RPMs the droplets remain levitated whereas for higher RPMs the droplets get deposited on the walls. This causes the airborne risk of infection all over the domain higher for low RPMs as compared to higher RPMs. Figure 23 depicting the spatial variation of risk over the domain paints the same story.

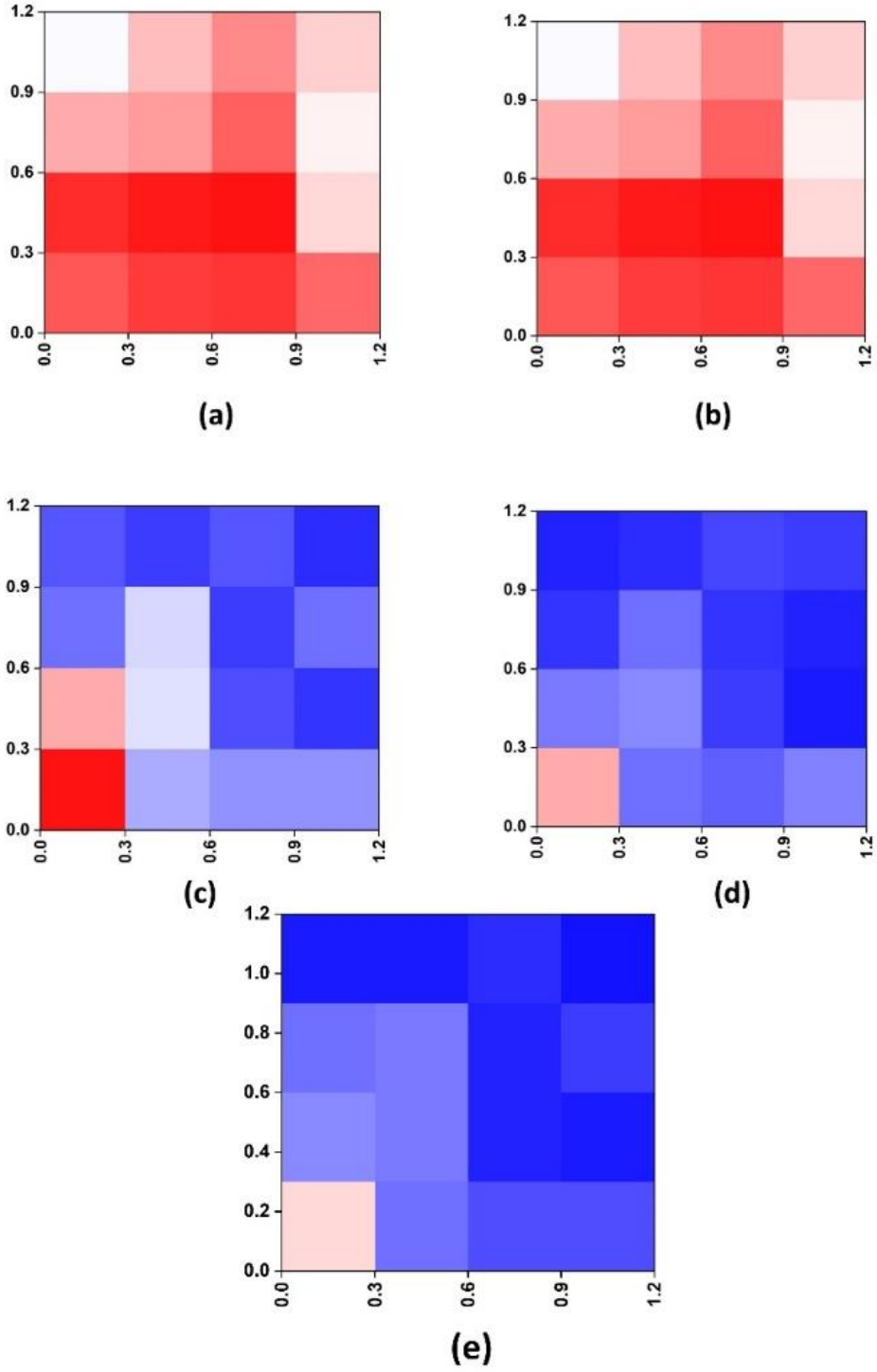

Figure 23: (a)-(e)Heat map showing the variation of risk of infection across the breathing boxes throughout the domain over the total exposure time for fan rpms 500,700,1000,1100,1200 respectively in a hot dry (30°C,50% R.H.) ambience.

Since a substantial percentage of droplets remain suspended in the domain near the mouth's height for low RPMs the infection risk increases in the domain as compared to quiescent domain where there is a orderly descent of the droplets. However, as the RPMs increase the risk decreases below that of the Quiescent ventilation scenario and beyond 1100 RPM there is no significant decrease, as depicted by spatio-temporal averaged risk of infection plot of Fig. 21. Thus 1100 RPM has been deemed to be minimum Fan speed that needs to be maintained.

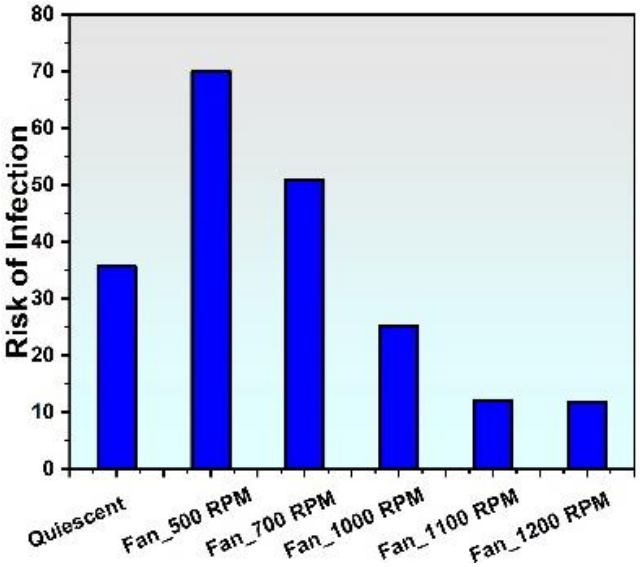

Figure 24: Comparison of spatio-averaged risk of infection between quiescent and various fan rpms in a hot dry (30ºC,50% R.H.) ambience.

For the Fan ventilation scenario, there is no such concentration of Risk in local regions as depicted by Fig. 25 for all ambiences. This is because in Fan ventilation scenario, due to the enhanced turbulence brought about by the rotational component of the fan, the droplets spread homogenously to various directions far away from each other and do not travel in a cluster (like they do in Quiescent scenarios). Furthermore, since a majority of droplets get deposited on the elevator surface rather than remaining suspended in the domain near the breathing box height as evidenced by Fig 18 (chapter 2), it ensures the fact that a significantly low risk is maintained across the enclosed domain for the Fan ventilation scenarios for all ambiences. Although the effect of climatic

ambience is much less profound in case of Fan ventilation the cold humid has lower infection risk as compared to a hot dry scenario as depicted by Figs 25 and 26. The risk of hot humid ambience lies in between that of cold humid and hot dry. This difference is brought about by the difference in evaporation characteristics for different ambiences. Since in cold humid and hot humid the droplets undergo negligible evaporation they settled down quicker due to their larger masses as compared to hot dry ambiences where there is a significant evaporation and generation of droplet nuclei.

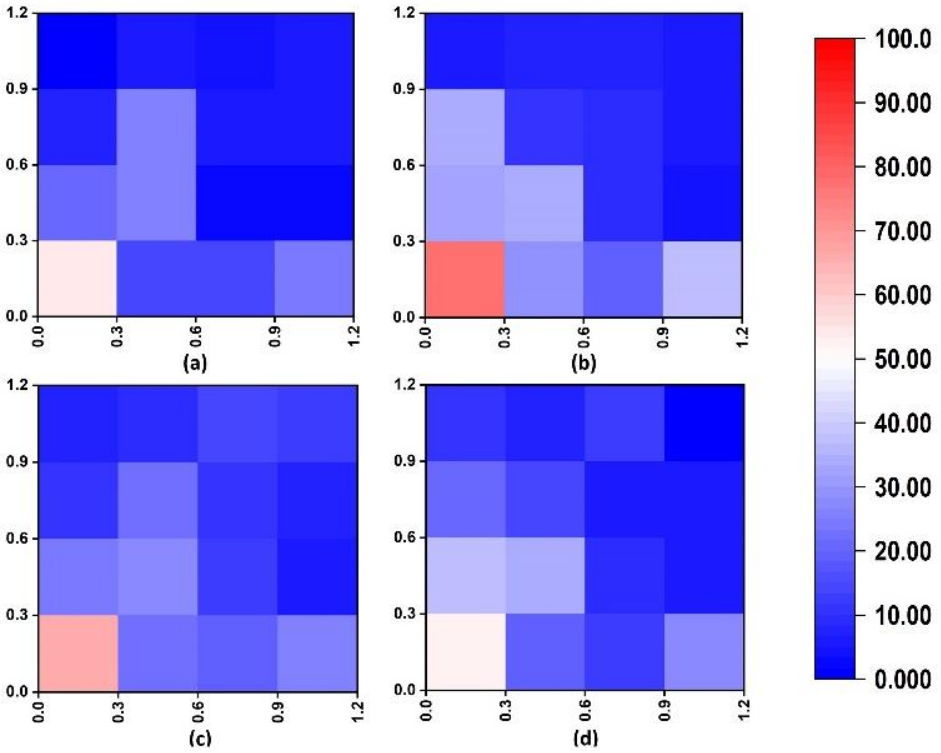

Figure 25 (a)-(d): Heat map showing the variation of risk of infection across the breathing boxes for fan ventilation scenario (1100 RPM) throughout the domain over the total exposure time for cold humid (15ºC,70% R.H.), hot dry (30ºC,30% R.H.), hot dry (30ºC,50% R.H.), hot humid (30ºC,70% R.H.) respectively.

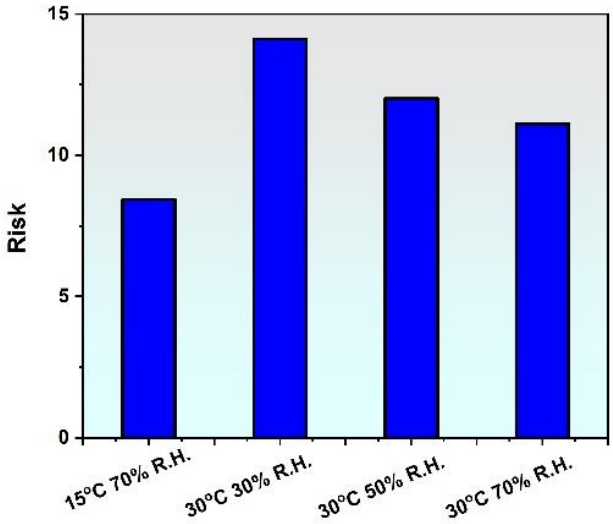

Figure 26: Showing the variation of spatio-averaged risk over the domain for various climatic ambiences for fan ventilation scenario (1100 RPM).

3.3. Epidemiological Implications of droplet size

We have studied epidemiological implications for various ventilation and climatic conditions and have quantified the spatial variation of the infection risk across the 16 breathing boxes, in various scenarios. The dose-response model quantifies the risk of infection based on the quantity of virion inhaled by a susceptible person. Up till now, all the studies have been based on the dose-response model. However, the severity and the ramifications of infection not only depend upon the number of virions inhaled but also significantly on the virion containing droplet size inhaled. Compared to a bigger droplet an evaporated smaller droplet containing the same virion quantity is more dangerous. The settling positions of the inhaled droplets vary within the respiratory tracts according to the size of the droplets. Smaller droplets, especially the virusols (droplet size < 20μm), may go into the alveolar and bronchial region but the larger ones may get arrested in the extrathoracic region[57]. If the droplets penetrate deep into the lower parts of the respiratory tract i.e., in the alveolar and bronchial regions, then the severity of the infection is significantly higher as compared to the droplets that get detained within the upper respiratory tract. Furthermore, infection in the lower part of the respiratory tract increases the risk of hospitalization and enhances the level of

possibility of clinical intervention in a person significantly[59]. The possibility of lasting damage to the respiratory system also increases significantly[59]. Furthermore, the size of virusols (droplet size < 20µm) cause them to linger in the domain for extended periods of time thus increasing the probability of inhaling them[75]. Additionally, the virion escape time is much less for small-sized droplets, the escape time is directly proportional to the droplet diameter, following which the speed of infection propagation is more in such types of droplets[76]. Hence, a detailed analysis pertaining to the Virusols (droplet size < 20µm) has been carried out.

The spatially averaged quantity of virusols (droplet size < 20µm) over the 16 breathing boxes as a percentage of suspended droplets (within the breathing boxes) for all time instants for all the climatic conditions for all the ventilation scenarios has been depicted in Fig.27. The cold humid condition (15^{o}C, 70% R.H.) does not produce any significant quantity of virusols and hence not been represented in the plot of Fig.27. Since the evaporation rate of droplets in hot-humid ambience is higher than that of cold humid ambience, a substantial proportion of suspended droplets are converted to Virusols (droplet size < 20µm) in hot-humid ambient environments for the quiescent scenario as depicted in Fig.27. The hot and dry ambient in a quiescent scenario produces a significant percentage of virusols (droplet size < 20µm), owing to their significantly high evaporation rates, as can be inferred from Fig. 27. This is due to the high evaporation rate in hot and dry ambient as evidenced by the diameter distribution plots in Figs. 11 and 17. However, the percentage of virusols (droplet size < 20µm) in the domain is low for all climatic ambient environments for fan ventilation because the percentage of suspended droplets in the breathing boxes within the appropriate height zone is inherently very low for the fan ventilation scenario in all climatic settings as can be seen from Fig. 27. Thus we conclude a quiescent hot dry ambient condition leads to the formation of a significant quantity of suspended virusols (droplet size<20µm). Droplets in hot and dry ambient due to their relatively smaller sizes as compared to the other ambience will have a greater deposition probability in the alveolar and bronchial regions. The probable particle deposition count in the

Extrathoracic region $D_{c_{ET}}$ and in the bronchial and alveolar region $D_{c_{BA}}$ within any breathing, box is quantified through a formulation as per equation 39.

$$D_{c_{ET}} = \langle \Sigma P_{i_{ET}} N_{D_i} \rangle_{B_j} , D_{c_{BA}} = \langle \Sigma P_{i_{BA}} N_{D_i} \rangle_{B_j} \quad (39)$$

; where N_{D_i} is the total number of particles of diameter D_i suspended within the breathing box B_j and $P_{i_{ET}}$ and $P_{i_{BA}}$ are the deposition efficiencies[57] in the Extrathoracic and bronchiolar and alveolar regions for that size of droplet respectively. Calculations using the above formulations are carried out for all the climatic conditions in a quiescent ventilation scenario. The respective temporally-averaged count of droplets within a breathing box that gets deposited within various parts of a respiratory tract, namely the Extrathoracic and the alveolar and Bronchial regions, are depicted in Fig. 28 for the Quiescent hot dry scenario. The cold humid, as well as the hot humid conditions, do not produce any droplets that might get deposited in the alveolar and bronchial regions. This is due to the fact that negligible evaporation occurs in the hot humid and cold-humid ambiences. On the other hand, extensive evaporation brought about by the hot dry ambience leads to the generation of a significant quantity of droplets that might get deposited in the alveolar and bronchial regions. The difference in evaporation characteristics and its impact on the evolution of the diameter of the suspended droplets has been depicted through the diameter ratio ($\frac{D_i}{D_i^0}$; D_i: diameter of the ith droplet at a certain time instant, D_i^0: Initial diameter of the corresponding ith droplet) the plot of Fig. 29. Thus, it can be concluded that the hot dry scenario not only produces the highest risk of infection but also increases the probability of infection severity by producing a significant quantity of droplets that can deposit in the lower parts of the respiratory tract.

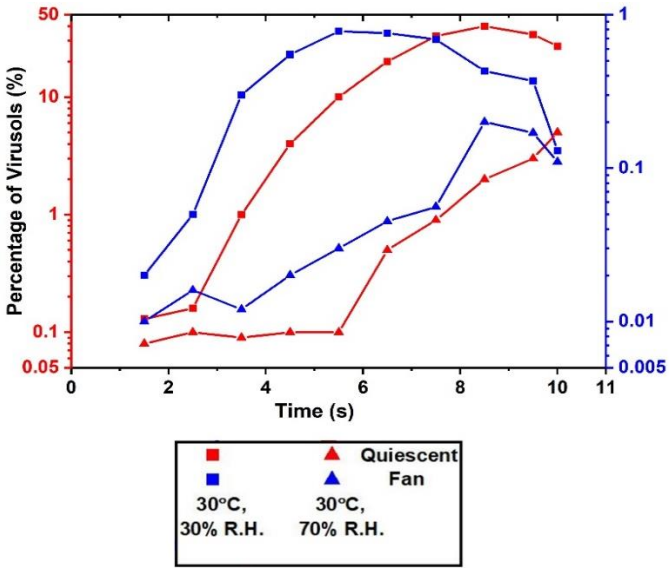

Figure 27: Plot showing quantity of Virusols (droplet size < 20µm) as percentage of suspended droplets for Quiescent and Fan ventilation scenario in various ambient environments.

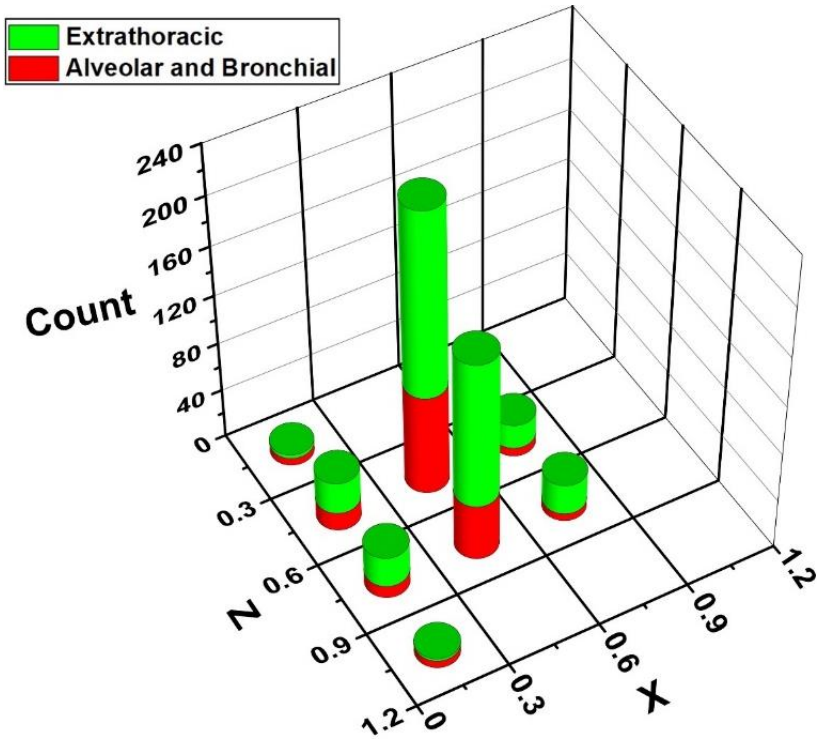

Figure 28: Depicting the temporally-averaged count of droplets within each breathing box that might get deposited in various parts of the respiratory tract in a quiescent ventilation scenario for a hot dry ambience(30°C,30% R.H.)

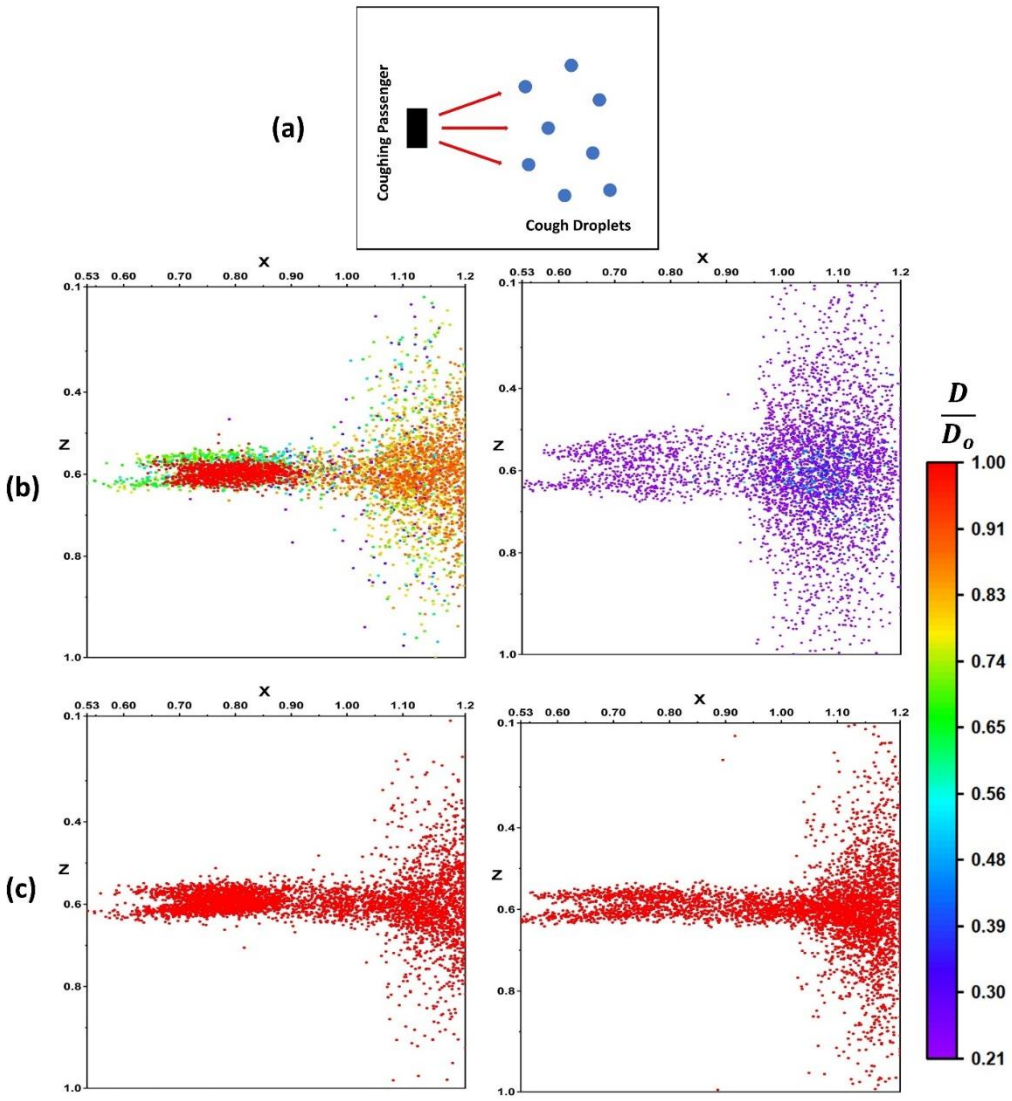

Figure 29(a): Schematic showing top-view of the coughing passenger emanating cough droplets into the domain.

(b-c): Plot showing Diameter ratio ($\frac{D}{D_0}$) of the cough droplets across the domain for quiescent scenario for hot dry condition (b) and cold humid condition (c) at various time instants.

3.4. Infection Transmission through the Fomite route.

The discussion on infection transmission so far has been focused solely on the airborne transmission route. However, one more equally significant route of transmission, i.e. the fomite route of infection transmission exists for the coronavirus[34]. Whenever pathogenic particles are deposited on solid surfaces,

the surfaces transform the particles into fomites. People who come into contact with these infectious surfaces may get the infection by transferring the pathogens through their hands. The droplet dispersion Fig.18 (chapter 2) clearly demonstrates that a significant percentage of injected droplets get stuck on the elevator surfaces, mainly for the fan ventilation scenario (multimedia view). Hence these situations present a risk of infection through an indirect contact transmission route. Without bringing these transmission routes into account, the risk analysis would be incomplete. Thus a thorough investigation of indirect transmission is indispensable in understanding the risk of infection.

The risk of fomite infection in each of the four elevator walls (left, right, front, and back as shown in Fig. 30) and its variation with height has been evaluated using the Nicas and Best model[77]**.** Owing to the significantly less decay rate on the elevator surfaces (assumed to be steel) Nicas and Best[77] model has been implemented (equations 40-42) using relevant literature data[77–79] and the assumption that a person touches the elevator surface once during the elevator travel time.

$$E_m = f_m c_m A_s \overline{C_{\text{hand},t_o}} t_o \tag{40}$$

$$\overline{C_{\text{hand},t_o}} = \frac{f_b c_h C_s}{(\varphi + f_h c_h + f_m c_m) t_0} \left[t_0 + \frac{\exp(-(\varphi + f_h c_h + f_m c_m) t_o) - 1}{\varphi + f_h c_h + f_m c_m} \right] \tag{41}$$

$$R = 1 - \exp(-\sigma E_m) \tag{42}$$

E_m being the dose of pathogen delivered to the mucous membrane, c_h is the pathogen transfer efficiency from the surface to the hand after a contact, c_m is the pathogen transfer efficiency from the hand to the mucous membrane after a contact, f_h is the frequency of hand-to-contaminated surface contact, f_m is the frequency of hand-to-mucous membrane contact, A_S is the average contaminated surface area touched per hand contact, t_o is the concerned time interval, C_s is the pathogen load per area of the contaminated surface, and φ is the decay rate of the pathogen on hand.

The fan ventilation scenario produces a significant fomite infection risk for all the ambiences, however, the change in ambient conditions does not bring about any change in the fomite infection risk. The air-flow pattern brought about by the Fan ventilation scenario at an RPM of 1100 dominates over all major changes brought about by climatic influences on droplet dynamics and hence there is no change in droplet dispersion in the fan ventilation scenario and subsequently on fomite risk with the change in climatic conditions, whereas on the other hand, the quiescent scenario in all ambiences produces negligible fomite infection risk as enumerated in Fig. 30. The walls are classified as left, right, front, and back with respect to the passenger inside the elevator who is facing the elevator door. The back wall (BW) and left wall (LW) pose the highest fomite risk of infection whereas the front wall (FW) and right wall (RW) present negligible fomite risk thus warning the passengers to avoid leaning on the back and right walls. The asymmetry between the left and right walls is mainly attributed to the flow circulation created by the anticlockwise fan rotation (as seen by the passenger from within the elevator). Hence, we conclude that although the fan ventilation scenario with 1100 RPM maintains significantly low risk through airborne transmission routes, it presents a substantial fomite transmission risk. Thus for the passengers, it is advised to take utmost precaution in abstaining from touching the walls as much as possible and to follow proper sanitization protocols after leaving the elevator.

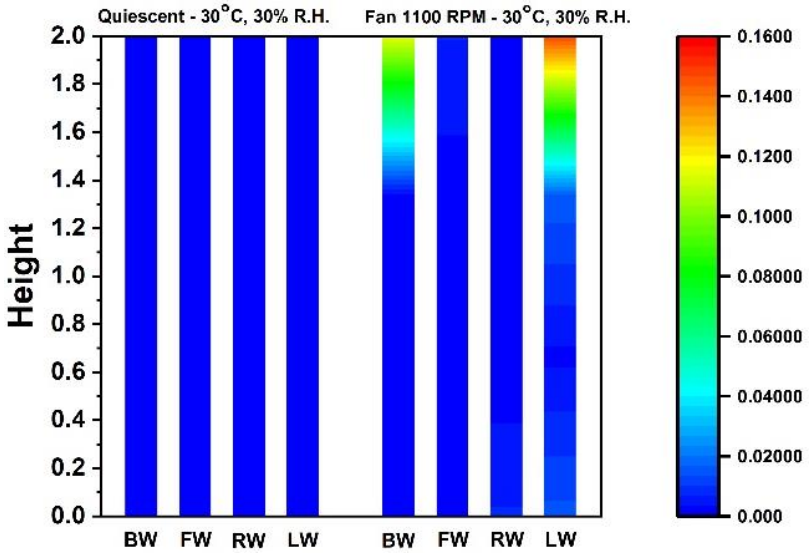

Figure 30: Contour plot showing the fomite risk variation with height on the elevator walls(BW: Back Wall, FW: Front Wall, LW: Left Wall, RW: Right Wall) for both quiescent and Fan ventilation scenarios.

3.5. Concluding Remarks

The dispersion and evaporation characteristics, and the epidemiological implications of ejected respiratory droplets in a small elevator commonly used in small buildings or enterprises have been studied. The effect of ventilation scenarios (Quiescent and Fan) as well as climatic conditions (Cold Humid, Hot Dry, Hot-Humid) on droplet dispersion and evaporation has been investigated. The proper Fan speed that ensures minimum risk in all climatic conditions has been determined.

A dose-response model has been implemented for investigating the spatial variation of airborne risk of infection in the domain based on the pathogen count within the breathing zone of a human (16 boxes, each of size 0.3m X 0.3m X 0.4m, at a height of 1.45m). The results suggest that a quiescent state in the elevator carries a very high risk because a substantial fraction of droplets stay suspended in the domain (especially in the vicinity of the human head), particularly in the hot dry condition (30℃, 50% R.H and 30℃, 30% R.H). The airborne risk of infection over the total exposure time was 35.68% and 36% for 30℃, 50% R.H and 30℃, 30℃% R.H ambient environments respectively. In contrast, the cold humid condition (15℃, 70% R.H) have a lower risk factor as

the droplets have larger masses throughout the travel time owing to negligible evaporation and quickly settle down below the height of the human breathing zone (risk of infection, 32%). The risk of infection in a hot humid ambient environment (30℃, 70% R.H) lies in between the cold humid, and hot dry ambient environments (risk of infection, 33%). The evaporation rate, although lower as compared to hot dry ambient, is higher in comparison to the cold humid environment. Hence comparing with a hot dry ambient environment, droplets descend quickly below the breathing zone height. However, since the evaporation rate is higher than a cold humid ambient environment, more droplets remain suspended in the domain. It was further established that although both temperature and humidity have a significant effect on the risk of infection, humidity has a more pronounced effect on the risk factor as compared to temperature.

The introduction of forced convection in the form of a fan, at proper fan speed, alleviates the condition for all climatic conditions. The Fan RPM of 1100 turns out to be successful in significantly lowering the airborne risk as compared to the quiescent scenario at all instants in the domain for all ambient conditions, by 8% to 14% for cold humid, and hot dry ambient environments respectively, and increasing the Fan speed beyond 1100 RPM does not yield significant risk reduction for any of the above climatic conditions. It was observed that at this fan speed of 1100 RPM, climatic influences cannot exert major changes in droplet dynamics and the risk arising out of this. Furthermore, it was noticed that although the Fan ventilation ensures a low airborne risk of infection in the domain, it increases the Fomite risk of infection significantly in all climatic conditions (Maximum risk of 16% in all climatic conditions) as compared to the quiescent scenario which has negligible fomite risk in all climatic conditions. Hence, although Fan ventilation needs to be maintained to minimize the more dangerous airborne risk of infection, precautionary measures involving avoidance of touching surfaces or an after-travel sanitization must be maintained to nullify the fomite risk.

Another important aspect that was investigated, was the development of small-sized droplets in the diameter range of less than 20 μm. These virusols (droplet

size<20μm), small-sized droplets with high viral loads have the highest penetration power in the alveolar and bronchial region of the respiratory tract and hence their transmission characteristics within the breathing boxes need to be investigated. In the quiescent ventilation scenario, the hot dry ambient environments due to their very high evaporation rate produce a significant quantity of Virusols (droplet size < 20μm) (24% of suspended droplets in the breathing zone at the end of 10s are virusols (droplet size<20μm)). The cold humid and hot humid ambient environments due to their significantly low evaporation rates produce negligible quantities of virusols (droplet size<20μm). The fan ventilation scenario due to the inherent low-risk factor produces a significantly low quantity of virusols (droplet size<20μm) in the breathing zone. The hot dry quiescent situation produces not only a situation with a very high likelihood of infection but also develops droplets of size ranges that have the maximum potential of penetrating into the bronchial and alveolar region. The spatial variation of the probable risk of infection in the extrathoracic as well as in the alveolar and bronchial regions of the respiratory tract has been thoroughly studied for all climatic ambiences in a quiescent ventilation scenario. The probable risk of infection in the alveolar and bronchial region for the cold humid and hot humid ambience is negligible whereas this type of infection risk is significant for hot dry conditions. Furthermore, for hot dry ambience, it has been concluded that the probable risk of infection in the alveolar and bronchial regions increases as one moves further from the afflicted person. Thus, one can safely conclude hot dry climatic ambient environment in a quiescent scenario is the most dangerous climatic condition in terms of covid transmission.

Chapter 4

Conclusions

In this study the droplet dynamics in an enclosed elevator has been investigated. The epidemiological implications of the droplet dispersion in the domain has been investigated. The effect of quiescent, Exhaust fan and Fan ventilation settings has been investigated on droplet dissemination. The implementation of forced circulation in the domain changes the droplet dynamics completely in the domain as compared to the quiescent scenario. The droplets follow an orderly descend in the quiescent scenario and a significant percentage of droplet remain suspended in the domain thus increasing the airborne infection risk. A stochastic dose response model has been implemented for quantifying the infection risk in the domain for various ambiences. The exhaust fan renders the domain completely safe as in 7.48s all the droplets escape the domain. In Fan ventilation scenario, at 1100 rpm, significantly decreases the percentage of droplet lingering in the domain as compared to the quiescent scenario, ultimately decreasing the airborne-infection risk completely. However, a significant droplet get deposited on the elevator surfaces thus increasing the Fomite risk significantly. The effect of ventilation in various climatic ambiences varying from cold humid (15℃, 70% R.H) to hot dry(30℃, 50% R.H and 30℃, 30% R.H) to hot humid (30℃, 70% R.H) has been investigated. A variation in airborne infection risk is observed across the ambiences. The lowest being in a cold humid and highest in a hot dry ambience owing to difference in evaporation characteristics in these ambiences with the risk in hot humid ambience lying between the cold humid and hot dry ambience. In cold humid and hot humid ambiences, the droplet undergo negligible evaporation and in hot dry ambiences the droplet undergo significant evaporation. In cold humid(spatio-averaged risk factor 30% over the exposure time of elevator travel time for a quiescent scenario), the droplets due their larger masses compared to hot dry owing to their evaporation characteristics descend quickly as compared to hot dry(spatio-averaged risk factor 42% for a quiescent) where droplets remain suspended in the domain due to their smaller masses due to the rapid evaporation in hot dry ambiences. The Fan ventilation scenario with 1100 RPM (having a spatio-averaged risk factor of 10%) decreases the risk of infection by 67% in a hot, dry

climatic condition as compared to a quiescent scenario. The Fan ventilation scenario (1100 RPM) is seen to sustain similar low risk irrespective of climatic variations. Although Fan ventilation scenario decreases the airborne risk, it increases the Fomite Risk, the maximum risk being 16%. The Fomite increases significantly from a quiescent (zero Fomite risk), since a significant fraction of injected droplets get deposited on the elevator surfaces.

REFRENCES

[1] Coronavirus: Mapping Covid-19 Confirmed Cases and Deaths Globally, https://www.bloomberg.com/graphics/2020-coronavirus-cases-world-map/ (accessed June 9, 2022).

[2] The COVID-19 pandemic will hurt long-term economic growth | IHS Markit, . https://ihsmarkit.com/research-analysis/the-covid19-pandemic-will-hurt-longterm-economic-growth.html (accessed June 21, 2022).

[3] It's Not Just SARS-CoV-2: Most Respiratory Viruses Spread by Aerosols, . https://ucsdnews.ucsd.edu/pressrelease/its-not-just-sars-cov-2-most-respiratory-viruses-spread-by-aerosols (accessed June 15, 2022).

[4] L. Bourouiba, E. Dehandschoewercker, J.W.M. Bush, Violent expiratory events: On coughing and sneezing, Journal of Fluid Mechanics. 745 (2014) 537–563. https://doi.org/10.1017/JFM.2014.88.

[5] M. Richard, J.M.A. van den Brand, T.M. Bestebroer, P. Lexmond, D. de Meulder, R.A.M. Fouchier, A.C. Lowen, S. Herfst, Influenza A viruses are transmitted via the air from the nasal respiratory epithelium of ferrets, Nature Communications. 11 (2020). https://doi.org/10.1038/S41467-020-14626-0.

[6] S. Basu, P. Kabi, S. Chaudhuri, A. Saha, Insights on drying and precipitation dynamics of respiratory droplets from the perspective of COVID-19, Physics of Fluids. 32 (2020). https://doi.org/10.1063/5.0037360.

[7] N. Sen, Transmission and evaporation of cough droplets in an elevator: Numerical simulations of some possible scenarios, Physics of Fluids. 33 (2021). https://doi.org/10.1063/5.0039559.

[8] Ansys Fluent Theory Guide 12, https://www.afs.enea.it/project/neptunius/docs /fluent/html/th/main_pre.htm (accessed June 20, 2022).

[9] H. Jasak, OpenFOAM: Open source CFD in research and industry, International Journal of Naval Architecture and Ocean Engineering. 1 (2009) 89–94. https://doi.org/10.2478/IJNAOE-2013-0011.

[10] T. Dbouk, D. Drikakis, On airborne virus transmission in elevators and confined spaces, Physics of Fluids. 33 (2021). https://doi.org/10.1063/5.0038180.

[11] L. Bourouiba, Fluid Dynamics of Respiratory Infectious Diseases, Annual Review of Biomedical Engineering. 23 (2021) 547–577. https://doi.org/10.1146/ANNUREV-BIOENG-111820-025044.

[12] L. Bourouiba, The Fluid Dynamics of Disease Transmission, Annual Review of Fluid Mechanics. 53 (2021) 473–508. https://doi.org/10.1146/ANNUREV-FLUID-060220-113712.

[13] J.P. Duguid, B. So, The size and the duration of air-carriage of respiratory droplets and droplet-nuclei, (1928). https://doi.org/10.1017/S0022172400019288.

[14] R. Pal, S. Sarkar, A. Mukhopadhyay, Influence of ambient conditions on evaporation and transport of respiratory droplets in indoor environment, International Communications in Heat and Mass Transfer. 129 (2021). https://doi.org/10.1016/J.ICHEATMASSTRANSFER.2021.105750.

[15] N. Buetti, P.H. Wicky, Q. le Hingrat, S. Ruckly, T. Mazzuchelli, A. Loiodice, P. Trimboli, V. Forni Ogna, E. de Montmollin, E. Bernasconi, B. Visseaux, J.F. Timsit, SARS-CoV-2 detection in the lower respiratory tract of invasively ventilated ARDS patients, Critical Care. 24 (2020) 1–6. https://doi.org/10.1186/S13054-020-03323-5/FIGURES/2.

[16] S.H. Ra, J.S. Lim, G.U. Kim, M.J. Kim, J. Jung, S.H. Kim, Upper respiratory viral load in asymptomatic individuals and mildly symptomatic patients with SARS-CoV-2 infection, Thorax. 76 (2021) 61–63. https://doi.org/10.1136/thoraxjnl-2020-215042.

[17] V.G. Melnikova, A.S. Epikhin, M. v. Kraposhin, The Eulerian–Lagrangian Approach for the Numerical Investigation of an Acoustic Field Generated by a High-Speed Gas-Droplet Flow, Fluids 2021, Vol. 6, Page 274. 6 (2021) 274. https://doi.org/10.3390/FLUIDS6080274.

[18] Y. Feng, T. Marchal, T. Sperry, H. Yi, Influence of wind and relative humidity on the social distancing effectiveness to prevent COVID-19 airborne transmission: A numerical study, Journal of Aerosol Science. 147 (2020). https://doi.org/10.1016/J.JAEROSCI.2020.105585.

[19] X. Li, Y. Shang, Y. Yan, L. Yang, J. Tu, Modelling of evaporation of cough droplets in inhomogeneous humidity fields using the multi-component Eulerian-Lagrangian approach, Building and Environment. 128 (2018) 68–76. https://doi.org/10.1016/J.BUILDENV.2017.11.025.

[20] Xia Yang, Hongyu Yang, Cuiyun Ou, Zhiwen Luo, Jian Hang, Airborne transmission of pathogen-laden expiratory droplets in open outdoor space, Science of The Total Environment, https://doi.org/10.1016/j.scitotenv.2021.145537.

[21] E. Maggiore, M. Tommasini, P.M. Ossi, Propagation in outdoor environments of aerosol droplets produced by breath and light cough, Https://Doi.Org/10.1080/02786826.2020.1847247. 55 (2020) 340–351.

[22] M. Aydin, · Fatih Evrendilek, · Ismail, E. Aydin, · Seckin, A. Savas, · Deniz, E. Evrendilek, Transport dynamics of SARS-CoV-2 under outdoor conditions, Air Quality, Atmosphere & Health 2022 15:5. 15 (2022) 893–899. https://doi.org/10.1007/S11869-022-01196-X.

[23] Y.-H. Cheng, E. Carolino, C.-C. Lin, F. Li, G. Jiang, T. Hu, Coughing Intensity and Wind Direction Effects on the Transmission of Respiratory Droplets: A Computation with Euler-Lagrange Method, (2022). https://doi.org/10.3390/atmos.

[24] R. Hetherington, A.B.M. Toufique Hasan, A. Khan, D. Roy, M. Salehin, Z. Wadud, Exposure risk analysis of COVID-19 for a ride-sharing motorbike taxi, Physics of Fluids. 33 (2021). https://doi.org/10.1063/5.0069454.

[25] T. Dbouk, D. Drikakis, On pollen and airborne virus transmission, Physics of Fluids. 33 (2021). https://doi.org/10.1063/5.0055845.

[26] S. Burgmann, U. Janoske, Transmission and reduction of aerosols in classrooms using air purifier systems, Physics of Fluids. 33 (2021). https://doi.org/10.1063/5.0044046.

[27] S.R. Narayanan, S. Yang, Airborne transmission of virus-laden aerosols inside a music classroom: Effects of portable purifiers and aerosol injection rates, Physics of Fluids. 33 (2021). https://doi.org/10.1063/5.0042474.

[28] M. Abuhegazy, K. Talaat, O. Anderoglu, S. v. Poroseva, K. Talaat, Numerical investigation of aerosol transport in a classroom with relevance to COVID-19, Physics of Fluids. 32 (2020). https://doi.org/10.1063/5.0029118.

[29] A. Foster, M. Kinzel, Estimating COVID-19 exposure in a classroom setting: A comparison between mathematical and numerical models, Physics of Fluids. 33 (2021). https://doi.org/10.1063/5.0040755.

[30] Y. Yan, X. Li, Y. Shang, J. Tu, Evaluation of airborne disease infection risks in an airliner cabin using the Lagrangian-based Wells-Riley approach, Building and Environment. 121 (2017) 79–92. https://doi.org/10.1016/J.BUILDENV.2017.05.013.

[31] H. Liu, S. He, L. Shen, J. Hong, Simulation-based study of COVID-19 outbreak associated with air-conditioning in a restaurant, Physics of Fluids. 33 (2021). https://doi.org/10.1063/5.0040188.

[32] Z. Zhang, T. Han, K.H. Yoo, J. Capecelatro, A.L. Boehman, K. Maki, Disease transmission through expiratory aerosols on an urban bus, Physics of Fluids. 33 (2021). https://doi.org/10.1063/5.0037452.

[33] X. Yang, C. Ou, H. Yang, L. Liu, T. Song, M. Kang, H. Lin, J. Hang, Transmission of pathogen-laden expiratory droplets in a coach bus, Journal of Hazardous Materials. 397 (2020). https://doi.org/10.1016/J.JHAZMAT.2020.122609.

[34] Y. Yang, Y. Wang, L. Tian, C. Su, Z. Chen, Y. Huang, Effects of purifiers on the airborne transmission of droplets inside a bus, Physics of Fluids. 34 (2022). https://doi.org/10.1063/5.0081230.

[35] F. Yao, X. Liu, The effect of opening window position on aerosol transmission in an enclosed bus under windless environment, Physics of Fluids. 33 (2021). https://doi.org/10.1063/5.0073171.

[36] J. Komperda, A. Peyvan, D. Li, B. Kashir, A.L. Yarin, C.M. Megaridis, P. Mirbod, I. Paprotny, L.F. Cooper, S. Rowan, C. Stanford, F. Mashayek, Computer simulation of the SARS-CoV-2 contamination risk in a large dental clinic, Physics of Fluids. 33 (2021). https://doi.org/10.1063/5.0043934.

[37] X. Li, C.M. Mak, K.W. Ma, H.M. Wong, Evaluating flow-field and expelled droplets in the mockup dental clinic during the COVID-19 pandemic, Physics of Fluids. 33 (2021). https://doi.org/10.1063/5.0048848.

[38] V. Mathai, A. Das, K. Breuer, Aerosol transmission in passenger car cabins: Effects of ventilation configuration and driving speed, Physics of Fluids. 34 (2022). https://doi.org/10.1063/5.0079555.

[39] D. Vernez, S. Schwarz, J.J. Sauvain, C. Petignat, G. Suarez, Probable aerosol transmission of SARS-CoV-2 in a poorly ventilated courtroom, Indoor Air. 31 (2021) 1776–1785. https://doi.org/10.1111/INA.12866.

[40] A. Cammarata, G. Cammarata, Dynamic assessment of the risk of airborne viral infection, Indoor Air. 31 (2021) 1759. https://doi.org/10.1111/INA.12862.

[41] A. Venkatram, J. Weil, Modeling turbulent transport of aerosols inside rooms using eddy diffusivity, Indoor Air. 31 (2021) 1886–1895. https://doi.org/10.1111/INA.12901.

[42] P.J. Drivas, P.A. Valberg, B.L. Murphy, R. Wilson, Modeling Indoor Air Exposure from Short-Term Point Source Releases, Indoor Air. 6 (1996) 271–277. https://doi.org/10.1111/J.1600-0668.1996.00006.X.

[43] X. Xie, Y. Li, A.T.Y. Chwang, P.L. Ho, W.H. Seto, How far droplets can move in indoor environments ? revisiting the Wells evaporation?falling curve, Indoor Air. 17 (2007) 211–225. https://doi.org/10.1111/j.1600-0668.2007.00469.x.

[44] S.L. Miller, W.W. Nazaroff, J.L. Jimenez, A. Boerstra, G. Buonanno, S.J. Dancer, J. Kurnitski, L.C. Marr, L. Morawska, C. Noakes, Transmission of SARS-CoV-2 by inhalation of respiratory aerosol in the Skagit Valley Chorale superspreading event, Indoor Air. 31 (2021) 314–323. https://doi.org/10.1111/ina.12751.

[45] Z.T. Ai, A.K. Melikov, Airborne spread of expiratory droplet nuclei between the occupants of indoor environments: A review, Indoor Air. 28 (2018) 500–524. https://doi.org/10.1111/ina.12465.

[46] C.H. Cheng, C.L. Chow, W.K. Chow, Trajectories of large respiratory droplets in indoor environment: A simplified approach, Building and Environment. 183 (2020) 107196. https://doi.org/10.1016/j.buildenv.2020.107196.

[47] A. Srinivasan, J. Krishan, S. Bathula, Y.S. Mayya, Modeling the viral load dependence of residence times of virus-laden droplets from COVID-19-infected subjects in indoor environments, Indoor Air. 31 (2021) 1786–1797. https://doi.org/10.1111/ina.12868.

[48] T. Dbouk, D. Drikakis, On respiratory droplets and face masks, Physics of Fluids. 32 (2020). https://doi.org/10.1063/5.0015044.

[49] K. Ashwini, A.K. Anjali, V. Sivaswamy, Role of aerosols in the spread of covid-19-a review, International Journal of Research in Pharmaceutical Sciences. 11 (2020) 1022–1025. https://doi.org/10.26452/IJRPS.V11ISPL1.3430.

[50] R. Biswas, A. Pal, R. Pal, S. Sarkar, A. Mukhopadhyay, Risk assessment of COVID infection by respiratory droplets from cough for various ventilation scenarios

inside an elevator: An OpenFOAM-based computational fluid dynamics analysis, Physics of Fluids. 34 (2022) 013318. https://doi.org/10.1063/5.0073694/5.0073694.MM.ORIGINAL.V3.MP4.

[51] Z. Peng, A.L.P. Rojas, E. Kropff, W. Bahnfleth, G. Buonanno, S.J. Dancer, J. Kurnitski, Y. Li, M.G.L.C. Loomans, L.C. Marr, L. Morawska, W. Nazaroff, C. Noakes, X. Querol, C. Sekhar, R. Tellier, T. Greenhalgh, L. Bourouiba, A. Boerstra, J.W. Tang, S.L. Miller, J.L. Jimenez, Practical Indicators for Risk of Airborne Transmission in Shared Indoor Environments and Their Application to COVID-19 Outbreaks, Environmental Science and Technology. 56 (2022) 1125–1137. https://doi.org/10.1021/acs.est.1c06531.

[52] Y. Guo, H. Qian, Z. Sun, J. Cao, F. Liu, X. Luo, R. Ling, L.B. Weschler, J. Mo, Y. Zhang, Assessing and controlling infection risk with Wells-Riley model and spatial flow impact factor (SFIF), Sustainable Cities and Society. 67 (2021). https://doi.org/10.1016/J.SCS.2021.102719.

[53] X. Shao, X. Li, ARTICLES YOU MAY BE INTERESTED IN, Phys. Fluids. 32 (2020) 115125. https://doi.org/10.1063/5.0032847.

[54] Z. Peng, A.L.P. Rojas, E. Kropff, W. Bahnfleth, G. Buonanno, S.J. Dancer, J. Kurnitski, Y. Li, M.G.L.C. Loomans, L.C. Marr, L. Morawska, W. Nazaroff, C. Noakes, X. Querol, C. Sekhar, R. Tellier, T. Greenhalgh, L. Bourouiba, A. Boerstra, J.W. Tang, S.L. Miller, J.L. Jimenez, Practical Indicators for Risk of Airborne Transmission in Shared Indoor Environments and Their Application to COVID-19 Outbreaks, Environmental Science and Technology. 56 (2022) 1125–1137. https://doi.org/10.1021/acs.est.1c06531.

[55] G.N. Sze To, C.Y.H. Chao, Review and comparison between the Wells-Riley and dose-response approaches to risk assessment of infectious respiratory diseases, Indoor Air. 20 (2010) 2–16. https://doi.org/10.1111/J.1600-0668.2009.00621.X.

[56] W. Liu, L. Liu, C. Xu, L. Fu, Y. Wang, P. v. Nielsen, C. Zhang, Exploring the potentials of personalized ventilation in mitigating airborne infection risk for two closely ranged occupants with different risk assessment models, Energy and Buildings. 253 (2021). https://doi.org/10.1016/j.enbuild.2021.111531.

[57] J.' Heyder, J. Gebhart, G. Rudolf, C.F. Schiller, W. Stahlhofen, DEPOSITION OF PARTICLES IN THE HUMAN RESPIRATORY TRACT IN THE SIZE RANGE 0.005-15/an, 1986.

[58] (3) Transfer of respiratory pathogens: Escape time of virions - YouTube, . https://www.youtube.com/watch?v=qjUR8WJWRgQ&list=PLUl4u3cNGP62-vPzt_GMdZRflJPjNdspG&index=9 (accessed May 15, 2022).

[59] COVID-19 Lung Damage | Johns Hopkins Medicine, . https://www.hopkinsmedicine.org/health/conditions-and-diseases/coronavirus/what-coronavirus-does-to-the-lungs (accessed May 17, 2022).

[60] S.Y. Ren, W.B. Wang, Y.G. Hao, H.R. Zhang, Z.C. Wang, Y.L. Chen, R.D. Gao, Stability and infectivity of coronaviruses in inanimate environments, World Journal of Clinical Cases. 8 (2020) 1391–1399. https://doi.org/10.12998/WJCC.V8.I8.1391.

[61] F.R. Menter, Two-equation eddy-viscosity turbulence models for engineering applications, AIAA Journal. 32 (1994) 1598–1605. https://doi.org/10.2514/3.12149.

[62] S.H. Smith, G.A. Somsen, C. van Rijn, S. Kooij, L. van der Hoek, R.A. Bem, D. Bonn, Aerosol persistence in relation to possible transmission of SARS-CoV-2, Physics of Fluids. 32 (2020). https://doi.org/10.1063/5.0027844.

[63] W. E. Ranz and W. R. Marshall, Evaporation from drops. Part II, Chem. Eng. Prog. 48 (1952) 173–180.

[64] W. E. Ranz and W. R. Marshall, Evaporation from drops. Part I, Chem. Eng. Prog. 48 (1952) 141–146.

[65] W. Sutherland, LII. The viscosity of gases and molecular force , The London, Edinburgh, and Dublin Philosophical Magazine and Journal of Science. 36 (1893) 507–531. https://doi.org/10.1080/14786449308620508.

[66] C.S. Ng, K.L. Chong, R. Yang, M. Li, R. Verzicco, D. Lohse, Growth of respiratory droplets in cold and humid air, Physical Review Fluids. 6 (2021). https://doi.org/10.1103/PHYSREVFLUIDS.6.054303.

[67] Bleier-FanHandbook, Fan Handbook, McGraw-Hill Education, 1998

[68] R. Leal da Silva, S.X. Brito Junior, L.L. S Simon, L.H. A Morais, R.E. P Silva, Characteristic Curves for a Ø500 mm Free Blow Fant and Its Energy Efficiency for INMETRO Standards and Overall https://www.researchgate.net/publication/263850565.

[69] E.A. Donoghue, ASME A17.1/CSA B44 Handbook ASME A17.1-2010, Safety Code for Elevators and Escalators CSA B44-10, Safety Code for Elevators, (2011).

[70] S. Dhawan, P. Biswas, Aerosol Dynamics Model for Estimating the Risk from Short-Range Airborne Transmission and Inhalation of Expiratory Droplets of SARS-CoV-2, Environmental Science and Technology. 55 (2021) 8987–8999. https://doi.org/10.1021/acs.est.1c00235.

[71] S. Basu, Computational characterization of inhaled droplet transport to the nasopharynx, Scientific Reports. 11 (2021). https://doi.org/10.1038/s41598-021-85765-7.

[72] Z. Zhang, T. Han, K.H. Yoo, J. Capecelatro, A.L. Boehman, K. Maki, Disease transmission through expiratory aerosols on an urban bus, Physics of Fluids. 33 (2021) 015116. https://doi.org/10.1063/5.0037452.

[73] A. Mikszewski, L. Stabile, G. Buonanno, L. Morawska, The airborne contagiousness of respiratory viruses: A comparative analysis and implications

for mitigation, Geoscience Frontiers. (2021). https://doi.org/10.1016/j.gsf.2021.101285.

[74] S. Anand, Y.S. Mayya, Size distribution of virus laden droplets from expiratory ejecta of infected subjects, Scientific Reports 2020 10:1. 10 (2020) 1–9. https://doi.org/10.1038/s41598-020-78110-x.

[75] C.E. Junge, Air Chemistry and Radioactivity, International Geophysics. 4 (1963).

[76] Transfer of respiratory pathogens: Escape time of virions - YouTube, . https://www.youtube.com/watch?v=qjUR8WJWRgQ (accessed May 29, 2022).

[77] M. Nicas, D. Best, A study quantifying the hand-to-face contact rate and its potential application to predicting respiratory tract infection, Journal of Occupational and Environmental Hygiene. 5 (2008) 347–352. https://doi.org/10.1080/15459620802003896.

[78] J.Y. Lee, J.W. Choi, H. Kim, Determination of hand surface area by sex and body shape using alginate, Journal of Physiological Anthropology. 26 (2007) 475–483. https://doi.org/10.2114/jpa2.26.475.

[79] H.A. Aboubakr, T.A. Sharafeldin, S.M. Goyal, Stability of SARS-CoV-2 and other coronaviruses in the environment and on common touch surfaces and the influence of climatic conditions: A review, Transboundary and Emerging Diseases. 68 (2021) 296–312. https://doi.org/10.1111/tbed.13707.